

Evaluating the Potential of Kode Technology to Attach Nucleic Acids onto Red Cells and Create Reticulocyte Mimics

Ashley Ronishma Naicker

A thesis submitted to Auckland University of Technology in fulfilment of the requirements for the degree
of Master in Medical Laboratory Science

2021

School of Science

Abstract

Reticulocytes are immature red cells that still have nuclei acid in them. They are an essential clinical indicator as an increase in their number indicates rapid turn-over of red cells. Most advanced automated haematology machines include a diagnostic assay for reticulocytes, and all diagnostic assays require quality control procedures. Herein lies the issue, sourcing cells suitable as controls for reticulocyte QC is problematic. Kode technology uses chemical constructs to modify cell surfaces with known quantities of small molecules. The opportunity exists to establish if human red blood cells can be labelled with Kode constructs that secondarily capture nucleic acids and create surrogate reticulocytes suitable for quality control.

This study aimed to investigate the potential to create reticulocyte controls prepared with Kode technology as an alternative to natural reticulocyte controls. Established methods were used to prepare biotin kodecytes and biotinylated DNA and these were attached to biotin-kodecytes via streptavidin. Due to limitations in materials, surrogates for biotinylated DNA were also used to evaluate steps designed to prepare mimic reticulocytes. A haematology analyser and supravital staining were used to assess the kodecyte mimic reticulocytes.

This research had partial success. DNA was successfully extracted, fragmented and biotinylated. Methods demonstrating that biotinylated polymers, including biotinylated DNA, could be attached to red cells coded with biotin via streptavidin bridge was also successful. However, the final product of mimic reticulocytes (biotin-kodecytes + streptavidin + biotinylated DNA fragments) was not successful.

Table of Contents

Abstract.....	ii
List of Tables	v
List of Figures	vi
Statement of Originality	vii
Acknowledgements	viii
1 Introduction.....	1
2 Materials and Methods.....	15
Reagents and Solutions	15
2.1 Preparation of DNA and Fragments.....	20
2.1.1 Samples and Methods for DNA Extraction	20
a. DNA Extraction using Buffers Prepared in house	20
b. DNA Extraction using Commercial Kit.	22
c. DNA Extraction using Proteinase K	23
2.1.2 Measurement of DNA Purity and Concentration	25
2.1.3 DNA Fragmentation	26
a. Sonication	26
b. Needle Shearing	27
2.1.4 Detection of DNA Fragmentation via Bioanalyser	27
2.2 Preparation of Biotinylated DNA Fragments	29
2.2.1 Detection of Biotinylation of DNA	30
2.2.2 Analysis of Biotinylated Polymer (Atri-PAA-Biotin) via Streptavidin-coated Plate	31
2.3 Preparation of Biotin-Streptavidin Kodecytes	36
2.3.1 Preparation of Streptavidin Kodecytes	36
2.3.2 Analysis of Ability of Avidin Kodecytes to Capture Biotinylated Polymer	37
2.4 Preparation of Biotin-Streptavidin- Biotinylated DNA Kodecytes.....	39
2.5 and Evaluating as Reticulocyte Mimic.....	39
2.5.1 Analysis of Mimic Reticulocytes by Aggregation	40
2.5.2 Analysis of Mimic Reticulocytes by Haematology Analyser	40
2.5.3 Analysis of Mimic Reticulocyte by Supravital Staining.....	41
3 Results.....	42
3.1 DNA Preparation and Fragmentation.....	42

Plant DNA extraction using buffers prepared ‘in-house’	42
DNA Extraction using Plant Extraction DNA Kit	45
DNA extraction Using Human Buffy Coat	46
3.1.1 DNA Fragmentation and Analysis- Human Buffy Coat	47
3.1.2 Analysis of Biotinylation of DNA via Agarose Gel	50
3.2 Validation of Biotinylated DNA Fragments	51
3.2.1 Results of the minimum concentration of biotinylated polymers.....	51
3.3 Validation of Biotin-Avidin Kodecytes.....	53
3.4 Evaluating Mimic Reticulocytes	54
3.4.1 Analysis of Mimic Reticulocytes by Haematology Analyser and Supravital Staining	55
4 Discussion	58
Reference	64
Glossary of Medical and Scientific Terms.....	73

List of Tables

Table 1: Maturation stages of reticulocytes.	4
Table 2: Protocol Parameters Used to Fragment Genomic DNA.	27
Table 3: Volumes for DNA biotinylation.	29
Table 4: Preparation of kodecytes and controls.	36
Table 5: Preparation of streptavidin kodecytes Atri-PAA-Biotin -Anti-A complexes.	39
Table 6: Sample preparation for mimic reticulocytes asses via Sysmex analyser.	41
Table 7: DNA extraction results from tomato leaves using Extraction buffer.	43
Table 8: DNA extraction results from tomato leaves using Edwards buffer.	43
Table 9: DNA extraction results (spinach leaves in Edwards buffer).	44
Table 10: DNA extraction results of undissolved DNA (spinach leaves in Edwards Buffer).	44
Table 11: DNA extraction results (stored tomato leaves).....	45
Table 12: DNA extraction results using the kit.	45
Table 13: DNA extraction results from spinach leaves using the kit.	46
Table 14: DNA extraction results from the human buffy coat by proteinase K method.	46
Table 15: Dilutions of unfragmented and fragmented DNA for Agilent 2100 Bioanalyser	47
Table 16: Fluorescent intensity excitation wavelength of 492 nm	52

List of Figures

Figure 1: Electron Scan Microscope image of normal reticulocyte.	2
Figure 2: Flow diagram showing present instrumentation and methodologies used.....	3
Figure 3: Supravital stained blood smear.....	5
Figure 4: Miller ocular micrometre disc.	6
Figure 5: Scattergram of reticulocyte channel in a haematology analyser.	9
Figure 6: Schematic representation of various Kode FSL constructs.....	12
Figure 7: FSL biotin construct.	13
Figure 8: Mimic reticulocyte.....	14
Figure 9: Image of a spin cartridge.....	23
Figure 10: Example output from Agilent 2100 Bioanalyser Electrophoresis.	28
Figure 11: Atri-PAA-Biotin (GlycoNZ) construct.	31
Figure 12: Modified sandwich Enzyme-Linked Immunosorbent Assay (ELISA) format.....	32
Figure 13: Modified ELISA format to detect varying concentrations of biotinylated samples	34
Figure 14: Doubling dilutions of Atri-PAA-Biotin and biotinylated DNA.	35
Figure 15: Doubling dilutions of biotinylated DNA.....	35
Figure 16: Kodecyte with Atri-PAA-Biotin polymer.	38
Figure 17: Column agglutination technology	38
Figure 18: Comparison of DNA pellet of Extraction buffer and Edwards’s buffer.	42
Figure 19: Electropherogram of unfragmented DNA extracted from human buffy coat.....	48
Figure 20: Electropherogram results of fragmented DNA extracted from human buffy coat.	49
Figure 21: Electropherogram results of fragmented DNA extracted from human buffy coat.	50
Figure 22: Gel-shift assay of biotinylated DNA-streptavidin dilutions via agarose gel electrophoresis	50
Figure 23: Colourimetric result of the reaction between enzyme streptavidin ALP and Atri-PAA-Biotin.	51
Figure 24: Colorimetric result of doubling dilutions of Atri-PAA-Biotin.....	52
Figure 25: Colorimetric result of varying concentrations of biotinylated DNA	Error! Bookmark not defined.
Figure 26: Column agglutination of streptavidin kodecytes.	54
Figure 27: Column agglutination of mimic reticulocyte.....	54
Figure 28: Sysmex analyser and BCB stain analysis.....	56

Statement of Originality

I hereby declare that the content of this submission is my own work and that, to the best of my knowledge and belief, it contains no material previously published or written by another person (except where explicitly defined in the acknowledgements), no material which is to a substantial extent has been submitted for the award of any other degree or diploma of a university or other institution of higher learning.

Sign:

Date: 08.06.2021

Acknowledgements

I would like to express my sincere gratitude to my primary supervisor Dr Holly Perry. Her dedication, keen interest and timely advice enabled me to complete my thesis. This journey would not have been possible without her continuous support and guidance. I am also thankful to my secondary supervisor Professor Stephen Henry whose expertise was invaluable throughout the research. His insightful feedback has sharpened my thinking and brought my research to a higher level.

I would like to thank Dr Nicolai Bovin, Dr Eleanor Williams, Senior Research Technician Timothy Lawrence for insights, directions, and technical assistance in experimental methods and critiquing my results.

I would like to thank Senior Laboratory Scientist Charlotte Hughes and the haematology laboratory staff at Middlemore hospital for the technical help in processing my research samples. I very much appreciate the assistance of Dr Jill Meyers in providing transport to and from the hospital and listening to my struggles and success in research along the way.

I am grateful to the staff and PhD students in the AUT Centre for Kode technology for the encouragement and guidance during my laboratory work. I have enjoyed and taken pride in being part of the Kode team.

I would like to thank my family and friends for the prayers and support throughout my studies.

1 Introduction

Reticulocytes

Since natural human red blood cells (RBC) only survive for 120 days, the human body is continually making new ones, approximately two million every second in healthy human adults^(1, 2). The immature RBCs are known as reticulocytes and are released from the bone marrow into the peripheral blood^(2, 3). They are formed from the differentiated haematopoietic stem cells (Burst Forming Unit-erythroid [BFU-E] and Colony Forming Unit-erythroid [CFU-E]) in the bone marrow, and the nucleus is ejected at the orthochromatic or late normoblast stage before becoming a reticulocyte^(2, 4, 5). The reticulocytes stay in the bone marrow to develop up to three days, after which they are released into the peripheral bloodstream with a life span of one day before maturing into an erythrocyte^(2, 4, 5).

Erythropoietin stimulates the bone marrow to increase the production of reticulocytes⁽²⁾. Maturation within the four days (bone marrow and peripheral blood) includes morphological, biochemical, and functional changes, leading to membrane remodelling, change in cell volume, the release of membrane-bound organelles and ribosomes⁽⁵⁾. A small amount of RNA remains in the reticulocytes, which is essential in the normal RBC maturation processes⁽⁵⁾. The International Council for Standardization in Haematology (ICSH) accepted the National Committee for Clinical Laboratory Standards (NCCLS) classification of reticulocyte as “non-nucleated red cell containing two or more particles of blue-stained material corresponding to ribosomal RNA”⁽⁶⁾. When scanned under an electron microscope, reticulocytes show irregular forms acquired by the cell membrane, as shown in Figure 1. Compared to mature RBC, lobular reticulocytes are larger, more deformable and less dense⁽⁵⁾.

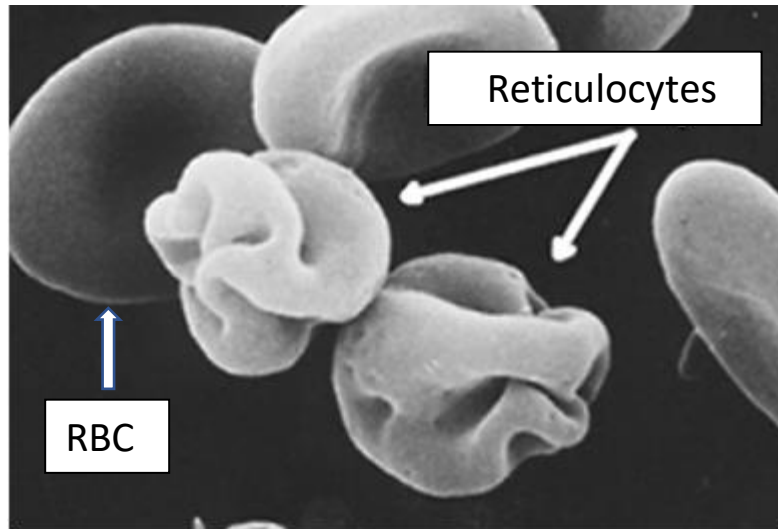


Figure 1: Electron Scan Microscope image of normal reticulocyte. The arrows indicate the lobular shape of the reticulocyte. Image adapted from Piva, Brugnara⁽⁵⁾.

Numerating reticulocytes in the peripheral blood is essential to assess if the bone marrow produces red blood cells effectively⁽⁷⁾. It helps in the differential diagnosis of anaemia and its classification. It is also an indicator for determining treatment success in patients with bone marrow aplasia or transplant, anaemia and recovery following therapy with drugs with marrow toxicity^(7, 8). A healthy individual should have a reticulocyte count between 0.5-to 2.5% of the total RBC count^(8, 9). The count depends on the bone marrow's erythropoietic activity and the rate at which the cells reach the peripheral blood from the bone marrow^(8, 9). Clinically, a high reticulocyte count (reticulocytosis) indicates that the bone marrow responds appropriately to anaemia and a lower count (reticulocytopenia) indicates its inability to respond^(8, 10).

Reticulocytosis is seen amongst anaemic patients with a functional bone marrow response to their anaemia⁽⁸⁾. Patients who suffer from blood loss have increased erythropoiesis; hence reticulocytosis is observed. Also, people who have disorders of the red cell membrane, including enzyme disorders, immune haemolytic disease, hypersplenism and haemoglobinopathies and suffer from haemolytic anaemia, have increased red cell destruction and a high reticulocyte count⁽⁸⁾.

In contrast, the mechanisms for reticulocytopenia or normal reticulocyte count despite anaemia include impaired haemoglobin synthesis and reduced erythropoiesis⁽⁸⁾. Such patients include those studied with vitamin B₁₂, folate and iron deficiency anaemia, leukaemia or metastatic carcinoma, immunologic or drug-induced red cell aplasia and renal failure^(8, 11, 12).

Apart from diagnostic value, reticulocyte measurements play a vital role in monitoring conventional or experimental drug therapy⁽¹³⁾. Haematology patients suffering from blood cancers receive recombinant

human erythropoietin (r-HU EPO) and other haematological growth factors to stimulate their erythroid production⁽¹³⁾. For example, a study that looked at r-Hu EPO use in neonatal anaemia stated that neonates who received r-Hu EPO showed a significant increase in reticulocytes indicating stimulation of erythropoiesis, thus correcting their anaemia and reducing the number of blood transfusions needed⁽¹³⁾. A similar result was seen in a study in which r-Hu EPO was administered to children with chemotherapy-induced anaemia^(14, 15). Both the studies showed a significant increase in reticulocytes, haemoglobin, and haematocrit in the treatment group, reducing the need for blood transfusion compared to the control group who did not receive the r-Hu EPO^(14, 15). Furthermore, r-Hu EPO, when administered in conjunction with oral supplements, reduces anaemia by stimulating erythropoiesis, especially among patients with refractory anaemia⁽⁸⁾.

In summary, the reticulocyte count is one indicator of an individual's erythropoietic status⁽²⁾. Traditionally, the sole purpose of reticulocyte count was to detect an increase in reticulocyte count in anaemia. However, with the rise in cytotoxic chemotherapy, bone marrow transplantation and irradiation, more precise counting of low reticulocyte counts is also required^(16, 17).

Enumeration of Reticulocytes

Historically, reticulocyte counts were performed using manual counts of cells infused with dye; however, several more modern techniques such as flow cytometry and image analysis are now available, as shown in Figure 2^(5, 8, 18).

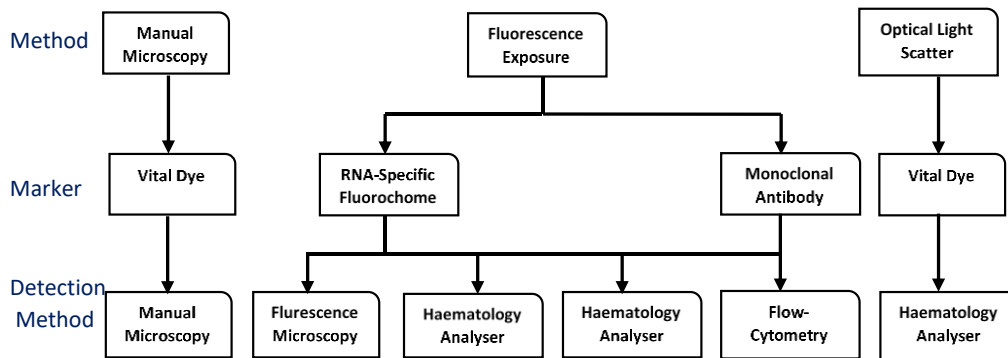


Figure 2: Flow diagram showing present instrumentation and methodologies used in laboratories for reticulocyte enumeration. Adapted from Riley, Ben-Ezra⁽⁸⁾.

In the late 1800s, a German researcher, Nobel Prize winner, and a visionary in haematology, Paul Ehrlich, utilised methylene blue to stain erythrocytes' microchemical structure in patients with pernicious anaemia^(5, 18). He described the stained material as subtle and dense content and thought that the basophilic material was a feature of a dying cell rather than a new cell^(5, 18). Other investigators from Germany, Italy, France, and North America confirmed this investigation and believed the stroma was evidence of the cell undergoing progressive coagulation necrosis^(5, 18, 19). In the early 1900s, the American bacteriologist Theobald Smith contradicted Ehrlich and stated that reticulocytes are immature erythrocytes^(5, 20). The term reticulocyte was first used by the renowned American medical society leader Edward Bell Krumbhaar, who observed erythrocytes showing reticulum through vital staining techniques⁽⁵⁾. In the same year, Smith stained red blood cells containing reticulum from cattle having pernicious anaemia⁽²⁰⁾. He used the supravital stain and concluded that these cells did not represent degenerative forms but rather “embryonic corpuscles, sent into circulation before their time to make good the losses going on”⁽²⁰⁾.

In the following century, Heilmeyer and Westhaeuser found evidence of various quantities of granular filamentous materials in RBC⁽¹⁷⁾. They classified reticulocytes into four stages of maturity. They provided the relative frequency at each step in the peripheral blood, as shown in Table 1, which laid the groundwork for the use of reticulocyte enumeration to guide clinical decisions⁽⁶⁾. In the last stage (Stage IV Table 1), the reticulocytes are found predominantly in the peripheral circulation, requiring correct interpretation.

Table 1: Maturation stages of reticulocytes. Classification according to Heilmeyer and quantification, according to Seip. Adapted from ^{Systemex} Educational Enhancement and Development ⁽⁶⁾.

Maturation stages, according to Heilmeyer	Morphological description	Quantification according to Seip (normal % of RBC)
Stage I	Reticulum consists of dense clots	< 0.1
Stage II	Loosely arranged reticulum	7.0
Stage III	Diffusely arranged reticulum	32.0
Stage IV	Some scattered granules	61.0

However, the cells can be mistaken for RBC due to the low RNA content, as shown in Figure 3^(6,9). When stained with Romanowsky stains, mature RBCs in a fixed blood smear stain salmon pink while immature RBC called polychromatic cells (in Romanowsky stain) stain bluish⁽⁵⁾. In supravital staining, RBC stains greenish-blue while reticulocytes stain greenish-blue with deep blue or blackish intracellular precipitates⁽⁵⁾.

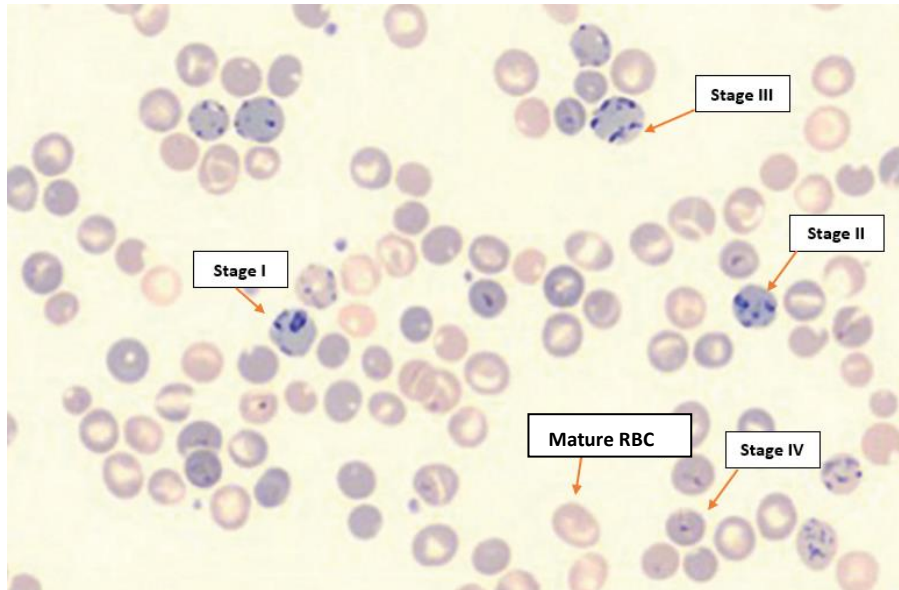


Figure 3: Supravital stained blood smear. The blood smear shows various stages of reticulocytes compared to mature reticulocytes. Adapted from Sysmex Educational Enhancement and Development ⁽⁶⁾.

In a conventional microscopic method, supravital stains such as New Methylene Blue (NMB) or Brilliant Cresyl Blue stain (BCB) and other cationic dyes are used to visualise the RNA remnants in reticulocytes⁽²¹⁾. The dye is added to a fresh aliquot of blood, and the dye crosses the reticulocyte membrane and binds to the RNA⁽²²⁾. Equal amounts of filtered stain and EDTA blood is aliquoted, homogenised and incubated for 10-30 minutes at room temperature⁽⁸⁾. Thin blood films are prepared on microscopic glass slides and examined under a light microscope using a 100× oil immersion objective⁽²³⁾. Approximately 1000 red cells are counted, and the percentage of reticulocytes is determined⁽²³⁾. Reticulocytes appear as RBC with basophilic (blue) stippling of the intracytoplasmic precipitate, either as a dot of small bluish-black granules or a mesh of blue reticular material⁽²⁴⁾. The reticulocytes are expressed as a percentage of the total RBC using the formula:

$$\text{Reticulocyte \%} = (\text{Number of Reticulocyte Counted per 100 RBC} \times 100) \div 1000.$$

An absolute reticulocyte count (ARC) is calculated using the formula:

$$\text{ARC} = \text{Number of RBC} \left[\times \frac{10^{12}}{L} \right] \times \text{Reticulocyte}(\%)^{(21, 23)}.$$

A Miller ocular micrometre disc can be used to reduce the number of erythrocytes counted from 1000 to a lower number. The disc has the advantage of standardising the area in which to estimate the red cells⁽²⁵⁾. The disc has two squares where the bigger square is nine times the smaller square area, as shown in Figure 4⁽²⁵⁾.

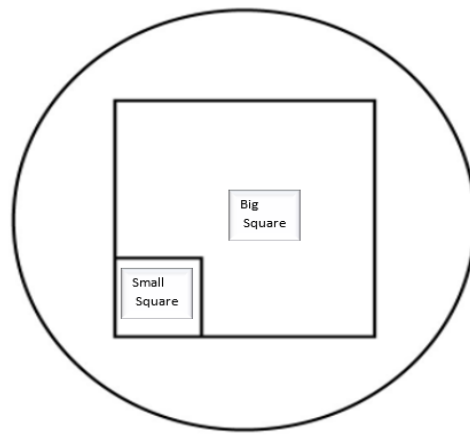


Figure 4: Miller ocular micrometre disc. Reticulocytes are counted in small and big squares, and RBC are counted only in the small square. Adapted from Sysmex Educational Enhancement and Development⁽⁶⁾.

The cells are counted at 100× objective with a 10× ocular secured with Miller disc⁽²⁵⁾. The reticulocytes are counted within the large square, including those touching the square's left and ruled bottom lines⁽²⁵⁾. RBCs are counted in the small square, whether they contain RNA or not⁽²⁵⁾. In the small square, reticulocytes are counted as an RBC and a reticulocyte⁽²⁵⁾. The count is continued until a minimum of 111 RBCs are observed, equivalent to 999 RBCs in a standard count mentioned earlier. The reticulocytes are expressed as a percentage of the total RBC using the formula:

$$\text{Reticulocyte \%} = (\text{Total Reticulocytes in Big Square} \times 100) \div (\text{Total RBC's in Small Square} \times 9)$$

An absolute reticulocyte count (ARC) is calculated using the formula:

$$\text{ARC} = \text{Number of RBC} [\times 10^{12} / \text{L}] \times \text{Reticulocyte}(\%)^{(25)}$$

Conventional counting methods are somewhat imprecise and can be affected by biological and pre-analytical variation in the laboratory. Firstly, pre-analytical issues of specimen collection, transportation and storage can affect the result^(8, 10). Whole blood collected in di/tri-potassium or disodium EDTA is utilised for reticulocyte count in the laboratories, while other anticoagulants are not currently used. In the

EDTA tube, reticulocytes' maturation continues *in vitro*; therefore, the sample should be processed within six hours if kept at room temperature or within 72 hours of collection if kept at 2-6°C^(8,10). Secondly, a well-stained smear with a uniform distribution of cells is ideal for reticulocyte count. However, the method of smear preparation (wedge smear or spun smear) can vary from person to person and result in less than ideal stained smear⁽⁸⁾.

Variability among trained scientists in identifying the morphology of reticulocytes is a further limitation of this method. It is difficult for scientists to differentiate between normal and low reticulocyte count during the early recovery of erythropoietic bone marrow activity⁽²⁶⁾. The relative count of reticulocytes could be misleading in cases where the red blood cell count is abnormal and bone marrow activity is stimulated in cases of anaemia. Therefore, an ARC needs to be calculated manually to correct for anaemia in the conventional method⁽²⁶⁾.

Other inaccuracies associated with manual counting include miscounting Pappenheimer bodies, siderotic granules, Heinz bodies, Howell-Jolly bodies, DNA remnants or haemoglobin H inclusions as RNA remnants^(8, 10). Due to the three main technical limitations in the reticulocyte detection, imprecision of manual microscopy method, and high coefficient of variation in counts (CV), the ARC has been somewhat underused in the clinical laboratory setting⁽²⁶⁾.

The use of immunofluorescence microscopy began in the early 1950s when Kozenow and Mai used nucleic acid-specific fluorochrome acridine orange to visualise nucleic acid⁽²⁴⁾. Following this discovery, other investigators used other ultraviolet-fluorescing dyes such as proflavine, 3,3'-diheptyloxycarbocyanine iodide (DiOCI), thioflavin T and pyronin Y^(8, 10). EDTA blood was fixed with formalin and stained with a dilute buffered dye such as acridine orange (AO), and reticulocytes were counted in a wet preparation on glass slides under a fluorescence microscope^(8, 10). Since this technique offered only similar results to light microscopy, and the fluorescence microscope is expensive, the immunofluorescence microscopy technique was not adopted by many^(8, 10).

With the introduction of modern haematology analysers in the early 1980s, the analysis of cells, including immature red blood cells, has become more sensitive and accurate. Typically manual methods analyse 1000 red blood cells, whereas modern haematological analysers process 7000-8000 cells within a short time frame to give more accurate blood cell counts of all types, including reticulocytes⁽²⁷⁾.

Over the subsequent years, flow-based cytometers used principles or combinations of principles based on light scatter, impedance, and conductivity by radio frequency⁽²⁸⁾. These instruments provided significant parameters that helped identify blood elements, including the maturation of reticulocytes⁽²⁸⁾.

The first principle applied in the diagnostic haematology analysers was the Coulter Principle or impedance measurement, named after the inventor, Wallace H Coulter⁽²⁹⁻³¹⁾. These analysers size and count the blood cells based on their electronic resistance whilst suspended in a conductive liquid (diluent) passing through a small aperture in a guided gentle vacuum⁽²⁹⁻³¹⁾. Blood cells function as electrical insulators when suspended in a conductive diluent. The dilute suspension of blood cells is drawn up through a small aperture⁽²⁹⁻³¹⁾. As the blood cells pass through the passage, individual blood cells briefly modulate the electrical path's impedance between the two submerged electrodes placed beside the aperture, creating an electrical impulse⁽²⁹⁻³¹⁾. The electrical impulses are directly proportional to the blood cell count, while the blood cells volume is directly proportional to the amplitude of the electrical impulse⁽²⁹⁻³¹⁾.

With the haematology analysers' development, reticulocyte count analysis is now available as part of the routine complete blood count analysis. Cell population data is generated for reticulocytes using the volume, conductivity, and light scatter analysis (VCS) of Beckman Coulter⁽³²⁾. The whole blood is incubated with a supravital stain such as new methylene blue in the haematology analyser. After the dye precipitates the RNA in the reticulocytes, a hypotonic clearing agent is added to clear the haemoglobin and unbound stain from the cells preserving the stained RNA within the cell⁽³²⁾. The younger reticulocytes have more residual RNA and stain more intensely than mature reticulocytes⁽³²⁾.

When illuminated with a helium-neon laser beam, younger cells scatter the most light. Mature reticulocytes have little residual RNA, and because of the clearing step with hypotonic solution, they are readily separated from mature red cells⁽²⁹⁾. The analyser determines the volume, conductivity, and light scatter of individual cells and plots them within a three-dimensional matrix⁽¹⁰⁾. Volume measures the size of the cell using direct current. Conductivity provides information about the cells with internal characteristics. The light scatters give information on the cell surface characteristics and cell granularity as they pass through the helium-neon laser beam⁽²⁹⁾. The immature reticulocyte will have more residual RNA and scatter more light than mature reticulocytes⁽²⁹⁾, while the mature RBCs and other cell differ from the stained reticulocytes by light scatter measurements, opacity appearances and direct current measurements⁽²⁹⁾.

Another principle utilised in haematology analysers, such as Sysmex analysers, is to count the circulating blood cells and their cellular components using three techniques. These are:

1. fluorescent flow cytometry with light scattering to measure RBC and differentiate the different type of White Blood Cell (WBC)^(6, 33, 34),
2. direct current impedance through hydrodynamic focusing for RBC and platelets^(6, 33, 34),
3. sodium lauryl sulphate (SDS) disruption of RBC for haemoglobin measurement^(6, 33, 34).

During flow cytometry, reticulocytes are counted by incubating the blood samples with a lysis reagent and a fluorescent dye (polymethine dye or thiazole orange). During the incubation, the cell membrane is punctured, and the fluorescent dye penetrates the cell and binds to the nucleic acid in the cytoplasm. Cells containing high amount of nucleic acids such as erythroblasts and leukocytes stain more intensely and are separated from reticulocytes with a lower nucleic acid amount^(6, 33, 34).

Reticulocytes analysed in this way use semiconductor laser light to detect forward scattering and side fluorescence as cells pass through an aperture^(6, 33, 34). When blood cells obscure the light, the light scatters from each cell in various directions. The forward light scattered is received by a photodiode, while laterally scattered light and the lateral fluorescent light are received by a photomultiplier tube^(6, 33, 34). The forward and lateral scattered light respectively provide information about blood cell size and the nucleus density. When light is emitted from fluorescent stained blood cells, light of a longer wavelength is produced. The fluorescent light intensity is increased with a higher content of RNA-stained reticulocytes^(6, 33, 34).

The forward light scatter, and fluorescence gives a bidimensional distribution presented as a scatter-gram showing mature red blood cells and reticulocytes (Figure 5)^(6, 33, 34).

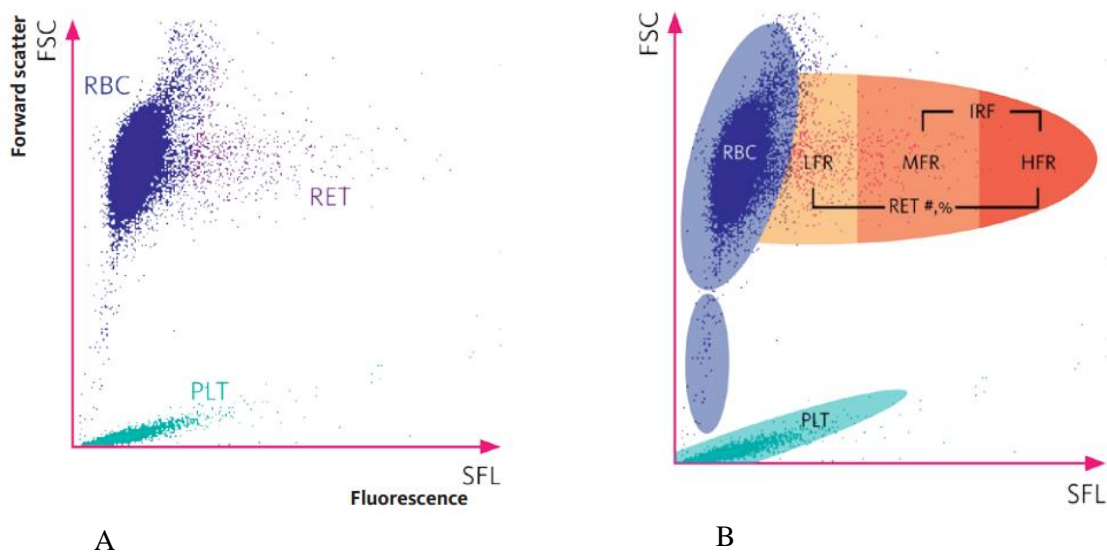


Figure 5: Scattergram of reticulocyte channel in a haematology analyser. In image A and B, the x-axis indicates fluorescent light intensity, and the y-axis shows forward scattered light. Image A dark blue cloud represents mature RBCs, and the purple scatter cloud right beside the blue cloud are reticulocytes (RET). The green cloud close to the x-axis represents the platelets. This image shows a normal scattergram of reticulocyte located near the mature RBCs. Image B shows the continuous non-separated distribution of reticulocyte maturation stages (LRF: Low Fluorescence Reticulocytes, MRF: Medium Fluorescence Reticulocytes, HFR: High Fluorescence Reticulocytes) depending on the fluorescence. Image copied from Sysmex Educational Enhancement and Development⁽⁶⁾.

Mature red cells contain no nucleic acid hence are easily distinguished from reticulocytes in the scatter plot. The reticulocytes are differentiated from the mature red blood cells based on their RNA levels as RNA is lost during differentiation into mature cells, as previously explained⁽³⁵⁾. Hence the reticulocytes are identified and counted within the red blood cells cohort based on their fluorescence intensity⁽³⁵⁾. The reproducibility of this assay is high⁽³⁵⁾. The analyser uses a threshold for the classification of cells, and the threshold depends on the intensity of the fluorescence and is divided into four fractions as shown in Figure 5: High Fluorescence Reticulocytes (HRF), Medium Fluorescence Reticulocytes (MFR), Low Fluorescence Reticulocytes (LFR), and RBC^(6, 33, 34). As the reticulocytes mature, they lose RNA, thereby facilitating the cells' division into the four fractions^(6, 36).

With the advent of automation, identifying and quantifying reticulocytes have become more reliable and accurate, providing credibility and clinical value^(26, 37). Automation has provided an opportunity to analyse approximately ten times more cells than manual methods, reducing inaccuracy and giving the reticulocyte count more credibility and clinical value^(5, 37, 38). Automation also eliminates the variability of smear staining, aliquoting stain and blood for dilution and incubation time^(5, 37, 38). Automation also enables a faster turnaround time with the opportunity for reflex reticulocyte count based on established algorithms^(5, 37, 38). Furthermore, automation eliminates the manual calculation of ARC and no longer requires correction for reduced haemoglobin concentrations⁽²⁶⁾. However, one complication when using these analysers arises from the difference in the reference intervals, which are strictly method and laboratory dependent^(26, 39, 40). Also, different automated methods use different reagents, which can present with different sensitivity to RNA and other cellular components⁽⁵⁾. In a study comparing three different reticulocyte enumeration methods, the authors concluded that the reticulocyte count varies significantly between automated haematology analysers using fluorescent dye thiazole orange and methylene blue dye⁽⁴¹⁾. Thus, monitoring patients across different laboratories becomes difficult, as method-specific reference methods cannot be interchangeably used⁽⁵⁾.

Existing Reticulocyte Quality Control

As with any laboratory method, reticulocyte enumeration requires controls for continuous monitoring of accuracy, reproducibility, and reliability. Reticulocyte controls are provided in different forms. It is difficult to use human blood as the source to prepare controls, as the reticulocyte is typically low to be useful in preparing a wide range of control levels⁽⁴²⁾. Furthermore, since reticulocytes undergo progressive maturation, the ability of the control material to give a reproducible reticulocyte count during storage is reduced⁽⁴³⁾. This problem has been largely overcome by including a fixation step to arrest

natural reticulocyte maturation⁽⁴³⁾. A three-level control is available from Beckman/Coulter Corporation (Retic-C) prepared from Avian RBCs and does not stain as the regular reticulocytes⁽⁴²⁾. Therefore the control is limited to use on Coulter automated haematology analysers. Several other commercial control kits such as *BIO-RAD Liquichek reticulocyte control (S)* and *BD retic-count* are available for the manual or instrumental count for reticulocytes⁽⁴³⁾. These reticulocyte controls are prepared from human blood components and provide a known reticulocyte count for the laboratory to measure their performance against⁽⁴³⁾. But commercial kits have drawbacks, for example, one commercial kit for reticulocyte quality control may not be compatible with all automated flow cytometers, may require special handling and may not reflect the very high or low reticulocyte count that can be seen in patient samples⁽⁴³⁾.

One of the methods in developing the reticulocytes is by harvesting reticulocytes from porcine blood by sedimentation, arresting maturation of reticulocytes, stabilising the harvested and arrested reticulocytes and preparing a predetermined concentration of the reticulocytes⁽⁴²⁾. Furthermore, the methods of making the reticulocyte control (as described in the U.S Pat. No. 5,432,089) involve encapsulating RBC with RNA by hypotonic lysis. At face value, these methods appear to be complicated, lengthy, and challenging to reproduce.

Kode Technology Opportunity

Kode technology is a surface attachment technology that allows biological and non-biological surfaces to be labelled with chemical constructs⁽⁴⁴⁾. The technology includes, but is not limited to, the labelling of human red blood cells with a wide variety of blood group antigens (including glycolipids), biotin and oligomers⁽⁴⁴⁾. Kode technology uses constructs that are both hydrophilic and hydrophobic (amphipathic) to harmlessly modify cell surfaces, allowing the cells to retain all their natural functions^(44, 45).

Properties of FSL Constructs

Kode technology is based on a unique and standard design known as Function-Spacer-Lipid (FSL)⁽⁴⁴⁾. Each FSL construct has three components (Figure 6): functional head, spacer and lipid tail⁽⁴⁴⁾. Each component can be individually designed and is interchangeable with different designs, leading to a specific biological function of each resulting FSL construct⁽⁴⁶⁾.

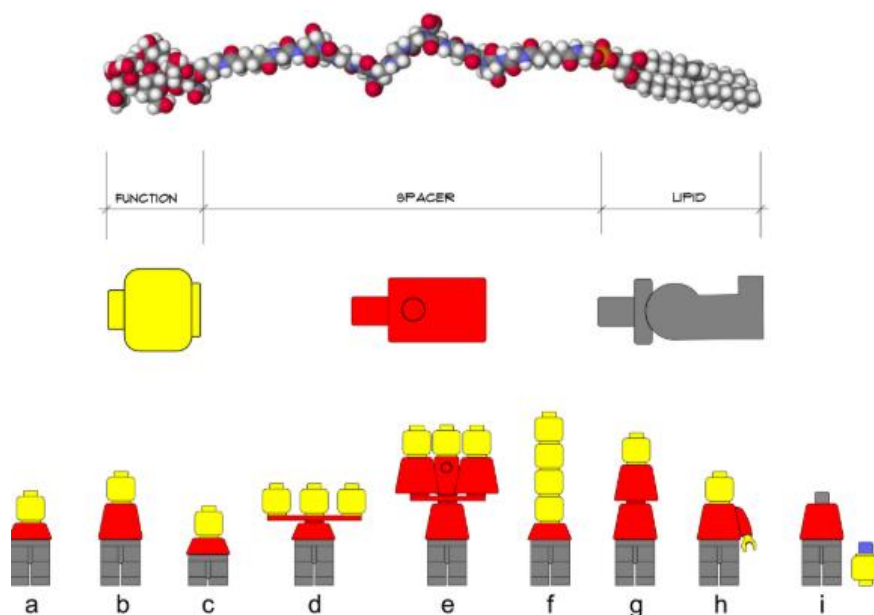


Figure 6: Schematic representation of various Kode FSL constructs. Building blocks figures illustrate the FSL constructs. The yellow block represents a functional head, red represents a spacer, and the grey block represents a lipid tail. Assembled building blocks a-i demonstrates the mix and match showing the flexibility of the FSL constructs. Figure copyright of Kode Biotech and reproduced with permission⁽⁴⁴⁾.

The hydrophilic functional “head” is the bioactive element of the construct and can be in the form of carbohydrates or peptides (for example, blood group antigens) or labels (for example, biotin)^(44, 45).

The biologically inert hydrophilic spacer carboxymethylglycine (CMG) is the central component of the FSL construct and differentiates the FSL from natural glycolipids^(44, 45). It spaces the functional group away from the surface membrane to enhance the bioactivity of the FSL, reducing the steric hindrance, thus increasing sensitivity and specificity when used in laboratory assays^(44, 45, 47). Furthermore, the spacer acts as a linker between the functional head and lipid tail and confers the water dispersibility property of the FSL. The water dispersibility property allows for ease of use with living cells^(44, 45). The spacers optimise the bioactivity or ligand binding with long (for example, 11.5 nm in CMG2), short (for example, 1.9 nm in Adipate), or branched forms of spacers^(45, 47). Since the spacer is biologically inert, it does not stimulate an immune response and does not cause cell toxicity⁽⁴⁷⁾.

The lipid “tail” at the end of the FSL construct is hydrophobic and acts similarly to a natural glycolipid, allowing the FSL to adhere naturally to the lipid-rich red cell membrane. Lipid to lipid attraction drives spontaneous self-assembly onto or into membranes. Overall, the FSL has an amphipathic character, as there is a hydrophilic functional head and hydrophobic lipid tail^(44, 45, 47). The lipid tail could be of various forms such as 1,2-O-distearyl-sn-glycero-3-phosphatidylethanolamine (DOPE), sterols such as cholesterol, and natural or synthetic ceramides⁽⁴⁷⁾. Kode technology harmlessly modifies cell surfaces,

allowing the cells to retain all biological functions⁽⁴⁸⁾. To date, FSL constructs have been used in various laboratory-based and clinical applications⁽⁴⁵⁾. When a cell surface modification is completed using FSL constructs, the resulting cell is called a kodeocyte^(45, 48). The FSL used in this study was FSL biotin, as it binds to another biotinylated polymer with streptavidin as a bridge (Figure 7).

Biotin-CMG(2)-Ad-DOPE

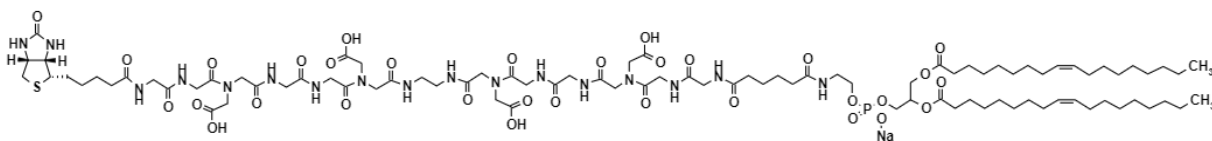


Figure 7: FSL biotin construct. It comprises a functional head of monomer biotin, conjugated to a CMG2 spacer carboxymethylglycine and a lipid tail of activated adipate of dioleoylphosphatidylethanolamine.

The concept of making “mimic reticulocytes” is to attach a nucleic acid onto the outside of mature human RBC using Kode technology (Figure 8). Although the outside will be labelled, they are still expected to mimic reticulocytes if the constructs aggregate on the surface.

The design was as follows:

- Biotin kodeocytes were prepared by incubating FSL biotin with mature human RBC⁽⁴⁹⁾
- Streptavidin was added in excess to bind to the biotin kodeocytes to produce “streptavidin kodeocytes”⁽⁴⁹⁾
- Human DNA was extracted from a buffy coat of whole blood and biotinylated using a commercial nick translation kit⁽⁵⁰⁾
- The streptavidin kodeocytes and biotinylated DNA were incubated together, utilising the principle that streptavidin has high affinity for biotin⁽⁴⁹⁾.
- To confirm the DNA’s attachment to the RBC, aggregation at the surface was anticipated. Routine reticulocyte methods of supravital staining and haematology analyser analysis were performed to assess the success in making mimic reticulocytes

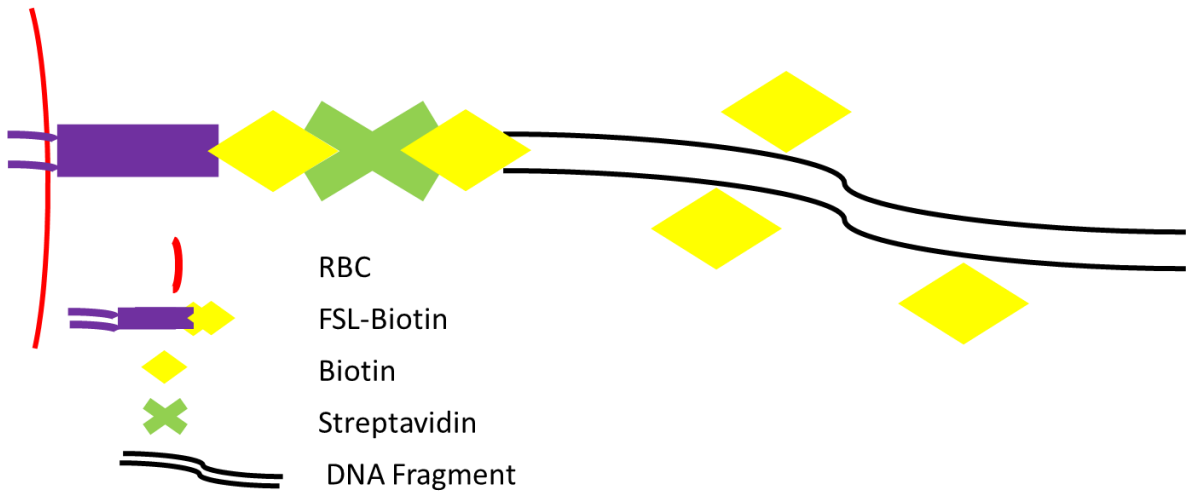


Figure 8: Mimic reticulocyte. The mimic reticulocyte is prepared by attaching FSL-biotin kodecytes to biotinylated human DNA via streptavidin as a bridge.

This study aimed to prepare mimic reticulocytes using Kode technology.

2 Materials and Methods

Reagents and Solutions*

Extraction Buffer (1% SDS, 0.5M NaCl)

1. Prepared 1% SDS by adding 1 g of SDS in 100 mL of distilled water.
2. Prepared 0.5M NaCl by adding 2.9 g of NaCl in 100 mL of distilled water.
3. The final buffer (1% SDS and 0.5M NaCl) was prepared by mixing entire volumes of reagents prepared in steps 1 and 2.

Edwards Buffer pH 7.5 (200 mM Tris, 0.5% SDS, 25 mM EDTA, 250 mM NaCl)

1. Prepared 200 mM of Tris by adding 2.4 g of Tris to 100 mL of distilled water, adjusted the pH to 7.8.
2. Prepared 0.5% SDS by mixing to 100 mL of distilled water.
3. Prepared 25 mM of EDTA by mixing 730 mg of EDTA to 100 mL of distilled water.
4. Prepared 250 mM of NaCl by mixing 1.46 g of NaCl to 100 mL of distilled water.
5. The final buffer ((200 mM Tris, 0.5% SDS, 25 mM EDTA, 250 mM NaCl) was prepared by mixing entire volumes of reagents prepared in steps 1-4.

RBC lysis buffer (150 mM NH₄Cl, 10 mM NaHCO₃, 0.1 mM disodium EDTA)

1. Prepared 150 mM of NH₄Cl by mixing 2 g in 250 mL of distilled water.
2. Prepared 10 mM of NaHCO₃ by mixing 210 mg in 250 mL of distilled water.
3. Prepared 0.1 mM of disodium EDTA by mixing 8.4 mg in 250 mL of distilled water.
4. The final buffer (150 mM NH₄Cl, 10 mM NaHCO₃, 0.1 mM disodium EDTA) was prepared by mixing entire volumes of reagents prepared in steps 1-3.

* Refer to Glossary of Medical and Scientific Terms for full names of the chemicals

WBC lysis buffer pH 8.0 (20 mM Tris-HCL, 0.1 mM disodium EDTA, 25 mM NaCl)

1. Prepared 20 mM of Tris by adding 600 mg in 250 mL of distilled water, adjusted pH to 8.0.
2. Prepared 0.1 mM of disodium EDTA by mixing 8.4 mg in 250 mL of distilled water.
3. Prepared 250 mM of NaCl by mixing 370 mg of NaCl to 100 mL of distilled water.
4. The final buffer was prepared by mixing entire volumes of reagents prepared in steps 1 to 3.

Tris-EDTA buffer (TE) pH 8.0

1. Prepared 10 mM of Tris by adding 300 mg in 250 mL of distilled water, adjusted pH to 8.0.
2. Prepared one mM of EDTA by adding 72.5 mg in 250 mL of distilled water.
3. The final buffer was prepared by mixing entire volumes of reagents prepared in steps 1 and 2.

10× Phosphate-Buffered Saline (PBS)

1. Added 160 g of NaCl, 4 g of KCl, 28.8 g of $\text{Na}_2\text{HPO}_4 \cdot 2\text{H}_2\text{O}$, 4.8 g of KH_2PO_4 in 1800 mL of distilled water.
2. The final buffer was prepared by adjusting the pH to 7.2 to the solution prepared in step 1 and adding distilled water to make the volume two litres.

1× Phosphate-Buffered Saline (PBS)

1. Added 200 mL of 10× PBS to 1800 mL of distilled water.
2. The final buffer (1× PBS) was prepared by adjusting the pH to 7.4 to the solution prepared in step 1.

10× Tris Borate Ethylenediaminetetraacetic acid (TBE)

1. Added 108 g of Tris base and 55 g of boric acid in 900 mL of distilled water.
2. Added 40 mL of 0.5 M of EDTA solution (pH 8.0) to step 1.
3. The final buffer was prepared by bringing the volume to one litre by adding distilled water to the reagents prepared in step 1 and 2.

0.5× Tris Borate Ethylenediaminetetraacetic acid (TBE)

Added 50 mL of 10× TBE to 950 mL of distilled water.

Tris Buffered Saline (TBS)

1. Added 6.06 g of tris, 8.77 g of NaCl, 0.2 g of MgCl₂ in 800 mL of distilled water.
2. The final buffer was prepared by adjusting the pH to 9.0 to the solution prepared in step 1 and adding distilled water to make the total volume one litre.

2% Bovine Serum Albumin (BSA)

Added 4 g of BSA to 199 mL of TBS and one mL of 10% sodium azide.

Substrate Buffer

1. Added 12.11 g of TRIS, 5.84 g NaCl, 10.15 g of Mg Cl₂. 6H₂O in 900 mL of distilled water.
2. The final buffer was prepared by adjusting the pH to 9.5 to the solution prepared in step 1 and adding distilled water to make the total volume one liter.

Proteinase K (20 mg/mL) (Thermo Fisher Scientific, Ambion,Cat # AM2546)

Diluted in 1:2 ratio with PBS to prepare 10 mg/mL of proteinase K.

1% Brilliant Cresyl Blue (BCB) in Citrate Saline

1. Dissolved 1 g of BCB and 0.4 g of sodium citrate in 100 mL of sodium chloride solution.
2. The final stain was prepared by mixing reagents in step 1 and storing the stain in a glass bottle at 4°C. The stain was filtered before use.

10% SDS

Prepared 10% SDS by adding 10 g in 100 mL of distilled water.

Ammonium acetate $\text{NH}_4\text{CH}_3\text{CO}_2$ (7.5 M)

Prepared 7.5 M of $\text{NH}_4\text{CH}_3\text{CO}_2$ by adding 289.06 g in 500 mL of distilled water.

Sodium Acetate NaCH_3COO (3 M)

Prepared 3 M of CH_3COONa by adding 61.52 g in 250 mL of distilled water.

Isopropanol (Fisher Scientific, Cat #: A451)

Absolute Ethanol (Fisher Scientific, Cat #: A962)

70% Ethanol (Fisher Scientific, Cat #: A962)

Added 100 mL of distilled water to 350 mL of absolute ethanol to make the final volume of 500 mL of 70% ethanol.

PureLink® Plant Total DNA Purification Kit (Thermo Fisher Scientific, Invitrogen Life Technologies, Cat #: K1830-01) containing binding buffer, wash buffer, elution buffer, spin cartridges and wash tubes.

Qubit™ dsDNA HS Assay Kit (Thermo Fisher Scientific, Invitrogen Life Technologies, Cat #: Q32851)

Qubit® assay tubes (Thermo Fisher Scientific, Invitrogen Life Technologies, Cat #: Q32856)

AMPure XP (Beckman Coulter, Cat #: A63882)

BioNick™ Labeling System kit (Thermo Fisher Scientific, Invitrogen™, Cat #: 18247-015)

Agilent High Sensitivity DNA Reagent (Agilent Technologies, Cat #: 0567-4627)

Streptavidin 5 mg/mL (ThermoFisher Scientific, Cat #: S888)

Streptavidin Protein, AP (ThermoFisher Scientific, Cat #: 21324)

FSL-CONJ (1Biotin)-SC2-L1 #187786 (Kode Biotech Materials Limited Cat #: 2153669)

ID-Cell Stab (*Bio-Rad*, Cat #: 005650)

Pierce™ Streptavidin Coated High-Capacity plates clear, 96-Well (ThermoFisher Scientific, Cat #: 15500)

PNPP Substrate (ThermoFisher Scientific, Cat #: 34045)

Atri-PAA-biotin (GlycoNZ, Cat #: 0085-BP)

CSL Anti-A (Epiclone, Cat #: 02611305)

LE Agarose (Thermofisher, Cat #: 14191220)

2.1 Preparation of DNA and Fragments

Although RNA is the nucleic acid present in reticulocytes, it was not practical for this research. The ribose sugar in RNA is more reactive due to hydroxyl bonding, whereas deoxyribose sugar in DNA has covalent bonds and is more stable in laboratory assays⁽⁵¹⁾. RNA is susceptible to degradation and also has a short half-life once extracted from tissues or cells due to RNases that degrade RNA⁽⁵¹⁾.

Genomic DNA is a double-stranded helical and can be extracted from any nucleated cell⁽⁵²⁾. To obtain reliable and quality results in downstream applications in this research, DNA extraction methods should achieve high DNA yield by removing impurities⁽⁵³⁾.

Two different methods utilising buffers prepared in this research (Extraction buffer⁽⁵⁴⁾ and Edwards buffer⁽⁵⁵⁾) were initially attempted with plant tissues. In addition, one commercial kit method was tested with plant tissues, and one “in-house” method with Proteinase K was tested with human blood.

2.1.1 Samples and Methods for DNA Extraction

The first experiments aimed to extract genomic DNA with minimum resources from fresh plant leaves. Two different methods with different buffers and different plant sources were compared.

a. DNA Extraction using Buffers Prepared in-house

For the initial extraction of plant DNA, tomato leaves were used. The leaves were procured from a home garden, put in a zip lock bag, and kept at 4°C until use. However, the tomato leaves wilted, and more were not available due to the winter season; therefore, tomato leaves were swapped for baby spinach leaves. Fresh leaves were preferred over wilted leaves as they have lower concentrations of secondary metabolites such as terpenes, phenolics or nitrogen-containing compounds and polysaccharides^(56, 57) and give higher purity and higher DNA yield as needed for this research. The spinach leaves were bought from the local supermarket and used for DNA extraction and kept at -20°C until use. They were preferred over tomato leaves due to their continued availability the whole year-round.

Extraction with Extraction Buffer (SDS, NaCl)

Approximately half a tomato leaf (0.5cm)² was ground using mortar and pestle with 400 µL of extraction buffer. An additional 100 µL of extraction buffer was added to help in grinding the leaf to a smooth pulp. The liquid containing coarse leaf particles was discarded, and 400 µL of residue was transferred to an Eppendorf tube. Additional extraction buffer was added to the tube to reach a volume of 1.2 mL. The tube was centrifuged at 21,300 g for four minutes at room temperature, after which 500 µL of supernatant was transferred to another Eppendorf tube. An equal volume of isopropanol was added to the supernatant, and the tube was mixed gently and placed on ice for five minutes. The tube was centrifuged at 21,300 g for four minutes at room temperature, and the supernatant was discarded. The resulting DNA pellet was washed in 500 µL of 70% ethanol, excess ethanol was discarded, and the DNA pellet was air-dried for one hour. Finally, the DNA pellet was resuspended in 50 µL of sterile water and stored at -20°C.

Extraction with Edwards Buffer (Tris, SDS, EDTA, NaCl)

Two medium-sized tomato leaves were ground and added to 400 µL of Edwards buffer in an Eppendorf tube using a mortar and pestle. The suspension was vortexed for 5 seconds and rested at room temperature for two minutes. The tube was then spun at 21,300 g for two minutes at room temperature. The supernatant (300 µL) was transferred to another Eppendorf tube, mixed with 300 µL of isopropanol, and left at room temperature for two minutes. The tube was centrifuged at 21,300 g for five minutes at room temperature, and the supernatant was discarded. The DNA pellet was washed in 500 µL of 70% ethanol and air-dried for one hour. The DNA pellet was resuspended in 100 µL of sterile water and stored at -20°C.

Method Modifications (Edwards Buffer)

The DNA pellet remained undissolved after resuspending in sterile water. As a result, all measurements for the purity and concentration were subsequently made on the supernatant, which meant that DNA concentration was underestimated because DNA in the Pellet was unavailable for measurement. Several extraction method modifications were made to resolve this problem: leaving the DNA pellet to dissolve overnight, placing the DNA pellet on the heat block (50°C) for four hours, reprecipitating the extracted DNA and switching isopropanol to ethanol during the precipitation stage⁽⁵⁸⁾.

b. DNA Extraction using Commercial Kit.

DNA extraction was performed using the PureLink® Plant Total DNA Purification Kit (Invitrogen K1830-01), following the kit manufacturer's instructions. The purpose of using the kit was to get relatively pure, high-quality DNA with minimal contamination, which had proved unattainable using the buffers (Edwards buffer and Extraction buffer). In addition, this kit allowed selective binding of DNA to the silica-based membrane in the presence of chaotropic salts⁽⁵⁹⁾. The plant material used for DNA extraction was tomato leaves and spinach leaves. All the reagents used for this method were provided in the kit (see Reagents and Solutions), and the steps were as follows:

Plant lysate preparation

Using a mortar and pestle, the leaves were ground and transferred to an Eppendorf tube. To the tube, 250 μL of resuspension buffer was added and vortexed to a homogenous lysate. To the lysate, 15 μL of 20% SDS and 15 μL of RNase A (20 mg/mL) was added, and the tube was incubated at 55°C for 15 minutes. The tube was spun at 21,300 g for five minutes to remove the insoluble material, and the clear lysate was transferred to another Eppendorf tube without disturbing the pellet. To the clear lysate, 100 μL of precipitation buffer was added and vortexed, and the tube was incubated on ice for five minutes. The tube was spun at 21,300 g for five minutes, and 250 μL of clear lysate was transferred into the PureLink® spin cartridge collection tube, as shown in Figure 9.

Binding DNA

To the clear lysate in the spin cartridge, 375 μL of binding buffer was added, and the spin cartridge was mixed by inverting. The cartridge was spun at 10,000 g for 30 seconds at room temperature. The flow-through was discarded, and the spin cartridge was placed into the dedicated wash tube provided in the kit.

Washing DNA

To the cartridge, 500 μL of wash buffer was added, and the cartridge was spun at 10,000 g for 30 seconds at room temperature. The flow-through was discarded from the wash tube, and the cartridge was placed back into the wash tube. This step was repeated twice. After the second spin, the cartridge was spun for 10,000 g for two minutes to remove residual wash buffer, and the wash tube was discarded.

Eluting DNA

The spin cartridge was transferred to an Eppendorf Tube, and 100 μL of elution buffer was added, and cartridge and tube were incubated at room temperature for one minute. The cartridge was centrifuged for one minute at 10,000 g , and eluted DNA was collected. The elution step was repeated in the same tube to recover more DNA. The cartridge was discarded after the last spin, whilst the eluted DNA was retained.

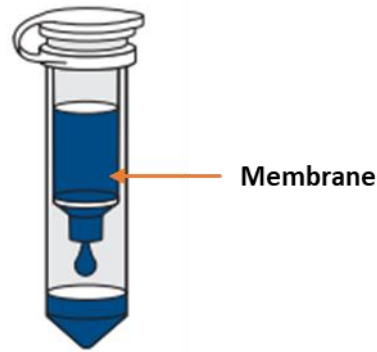


Figure 9: Image of a spin cartridge as used in the PureLink Plant Total DNA Purification kit. Fluid is shown dripping through the cartridge, whereby DNA binds to the silica-based membrane.

Storing DNA

The DNA was stored at either 4°C or -20°C depending on the usage time. DNA stored at 4°C was used in further experiments within 48 hours, whereas -20°C was used for longer storage times⁽⁶⁰⁾.

Method Modifications

The kit method was used several times to extract DNA as the DNA concentration from single runs was low. Using fresh baby spinach leaves, a single extraction yield of 2.3 ng was obtained; however, this was insufficient for downstream application. To get a higher DNA concentration, the second elution step was carried out using a lower volume (50 µL) of elution buffer (instead of 100 µL); however, the yield was still insufficient. Thus, even with multiple extractions, the kit would not have provided sufficient DNA for downstream application.

c. DNA Extraction using Proteinase K

Blood samples were collected from two healthy laboratory volunteers in ethylenediaminetetraacetic acid (EDTA)-containing vacutainers.

A total of six EDTA tubes of approximately six mL of blood were collected. Fresh samples were spun at 300 g for 10 minutes, and the buffy coat (white blood cells and platelets) was removed from the separated blood samples to individual 15 mL sterile plastic tubes. The samples were processed for DNA extraction within 12 hours of collection.

The extraction procedure is divided into three parts: RBC removal and lysis, WBC lysis and protein removal and DNA extraction, following a published protocol⁽⁵⁰⁾.

RBC lysis and removal

The buffy coat from EDTA samples was removed and mixed with 8 mL of RBC lysis buffer. After manually inverting the tubes for five minutes to mix the buffy coat and RBC lysis buffer, the tubes were centrifuged at 300 g for 10 minutes. The supernatant containing lysed RBC was decanted manually, leaving the WBC pellet at the bottom of the tube. To the pellet, 500 μ L phosphate-buffered saline (PBS) was added. The lysis and removal processes were repeated three times, and after the third step, the clean white pellet was resuspended in 500 μ L PBS.

Method Modifications

In modifications to the published protocol⁽⁵⁰⁾, a buffy coat instead of whole blood was used.

WBC lysis and protein removal

To the white cell pellet suspended in 500 μ L of PBS, 1.5 mL of WBC lysis buffer, 500 μ L of 10% SDS and 50 μ L proteinase K was added. The mix was incubated in the water bath at 50°C for two hours or until the pellet dissolved (on some occasions, up to two and a half hours). In a few tubes, the white cell pellet did not dissolve in two and a half hours; therefore, another 500 μ L of SDS and 50 μ L of proteinase K was added and re-incubated for 15 minutes when the pellet dissolved.

DNA extraction

The tubes were cooled down to room temperature after incubation at 50°C. To the mix in the tubes, 500 μ L of 7.5M of ammonium acetate was added and vortexed gently till the solution was homogenised. Seven mL of chilled absolute ethanol (stored at -20°C) was added. The tubes were inverted until DNA strands were visible and condensed in appearance. Nichrome wire loops were flamed and cooled before being used to collect the DNA. The loop full of DNA was transferred to 1.5 mL Eppendorf tubes and washed twice in 500 μ L of 70% ethanol. Ethanol was decanted and left to evaporate at room temperature for approximately 30 seconds. Once the ethanol evaporated, 200-400 μ L of TE buffer was added. The TE buffer amount depended on the observed DNA's size, with more TE buffer added to the larger pellets. The tubes were incubated in a water bath at 37°C till the DNA pellet dissolved. All samples were stored at 4°C overnight and later at -20°C for future use.

It was noted that the DNA was still viscous after leaving overnight, and this may have been due to too much DNA for the amount of TE buffer⁽⁵⁰⁾. Therefore, another 200 μ L of TE buffer was added to all samples on the following day, and tubes were gently vortexed. The concentration and purity were measured. However, in some tubes, DNA was still viscous and was left at room temperature for a few hours, after which concentration and purity were measured. The tubes in which DNA had dissolved showed high DNA

concentration (350-420 ng/ μ L); however, the tubes with slight viscosity had lower concentration (140-150 ng/ μ L), presumably due to undissolved DNA not being available for measurement.

2.1.2 Measurement of DNA Purity and Concentration

Two different methods were utilised to measure DNA purity and concentration: Ultraviolet spectrophotometry (NanoVue) and fluorometry (Qubit).

UV spectrophotometry (NanoVue) provides a valuable way of determining the purity and concentration by measuring the maximum absorbance of nucleic acid in the samples. DNA and RNA maximally absorb light at 260 nm, while protein absorbs at 280 nm, and the ratio of nucleic acid to protein (A_{260}/A_{280}) indicates the purity of DNA in the sample⁽⁶¹⁾. It allows quantification of both single and double-stranded DNA and proteins; however, the DNA concentration can be falsely elevated due to inference of proteins, single nucleotides, and DNA fragments^(62, 63).

Before measuring the samples, a spectrophotometry blank was performed using 2 μ L of distilled water or TE buffer (whichever solution the DNA was dissolved in). Once the NanoVue was blanked, two μ L of the DNA sample was placed onto the instrument's pedestal, and the DNA concentration and A_{260}/A_{280} ratio were recorded.

Fluorometry (Qubit) quantifies DNA based on the fluorescence intensity of a fluorescent dye, which binds to nucleic acids, with the resulting fluorescence intensity being proportional to the quantity of nucleic acid⁽⁶⁴⁾. A QubitTM 2.0 Fluorometer (Thermo Fisher Scientific) double-stranded DNA High Sensitivity Assay (Thermo Fisher Scientific) was used according to the manufacturer's protocols⁽⁶⁴⁾. The assay is highly selective for DNA over RNA and quantitates samples with concentrations between 10 pg/ μ L to 100 ng/ μ L⁽⁶⁴⁾. The working solution was prepared by diluting the QubitTM dsDNA HS reagent with the QubitTM dsDNA HS buffer (with the volume-dependent upon the number of samples)⁽⁶⁴⁾. In two separate tubes, 190 μ L of Qubit working solution was added to 10 μ L of QubitTM dsDNA HS standard # 1 and QubitTM dsDNA HS standard # 2 vortexed for two to three seconds⁽⁶⁴⁾. Standards # 1 and # 2 aid in judging the analyser's performance and whether the test samples are within the specified concentration range. In another tube, 198 μ L of Qubit working solution was added to two μ L of the sample containing DNA and vortexed for two to three seconds. All tubes were incubated at room temperature for two minutes⁽⁶⁴⁾. During the incubation time, the fluorescent dye (PicoGreen) binds to the bases and becomes intensely fluorescent. As a result, the fluorescence intensity is directly proportional to DNA concentration in the sample without interference from other molecules such as RNA and proteins⁽⁶⁴⁾.

DNA measurements by fluorometry allowed precise nucleic acid measurements and allowed more sensitive measurements in low concentration DNA samples than the NanoVue spectrophotometric measurement of DNA⁽⁶²⁻⁶⁴⁾. However, Qubit measurement did not provide any information on the purity of the sample and was not suitable for higher DNA concentration samples extracted from human buffy coats. Therefore, both spectrophotometry (NanoVue) and fluorometry (Qubit) were used at different times throughout this research.

2.1.3 DNA Fragmentation

To later biotinylate DNA, it was considered necessary to break up the genomic DNA extracted from the human buffy coat into smaller fragments⁽⁶⁵⁾. DNA was fragmented using two methods: sonication (Covaris M220) and needle shearing.

a. Sonication

The Covaris M220 focused-ultrasonicator (Covaris, USA) was used for genomic DNA fragmentation using 300bp and 500bp fragment protocols. The Covaris uses Adaptive Focused Acoustics (AFA) technology operating at 500 kHz. Due to its short wavelength, the ultrasonic acoustic energy is focused on the sample^(66, 67). The emitted ultrasonic energy focused on the samples is achieved with a concave transducer^(66, 67). The Covaris tubes, which contain the sample (DNA for this research), are exposed to the active acoustic focusing, allowing the energy to shear DNA to form fragments, with the average fragment size specified^(66, 67). The Covaris tubes are immersed in a water bath to maintain isothermal conditions. Other parameters such as treatment time, cycles per burst, peak incident power have been optimised as established per protocols to precisely attain the burst of ultrasound energy^(66, 67).

The genomic DNA was diluted before loading into the 130 μ L Covaris tube to meet the concentration range specified for Covaris. The ratio of DNA to water was calculated as:

$$\text{Amount of DNA} = 5000 \text{ ng} (\text{DNA input in the } 130 \mu\text{L tube}) \div \text{DNA concentration}$$

Appropriate temperature, cycles per burst and treatment time were selected with each fragment size protocol shown in Table 2.

Table 2: Protocol Parameters Used to Fragment Genomic DNA.

Parameters		
Target base pair peak	300	500
Temperature (°C)	20	20
Cycles per burst (cpd)	200	200
Treatment time (sec)	65	50

b. Needle Shearing

Needle shearing creates DNA fragments as genomic DNA is passed through the small gauge of a needle. By passing the genomic DNA multiple times through the needle gauge, the DNA physically shears into fragments⁽⁶⁸⁾. This method was attempted as a low-cost alternative to ultrasonication.

A 27-gauge needle was attached to an insulin syringe, and the tip of the needle was placed into the bottom of the Eppendorf tube. The Eppendorf tube contained genomic DNA (125 ng/ μ L) dissolved in 200 μ L of TE buffer. The plunger was pulled till all the liquid was drawn from the bottom and expelled back into the tube. This step was repeated ten times.

2.1.4 Detection of DNA Fragmentation via Bioanalyser

The Agilent 2100 Bioanalyzer is a platform based on microfluidics that aids in quantifying and sizing nucleic acids through electrophoretic separation⁽⁶⁹⁾. It is based on gel electrophoresis, performed on a capillary electrophoresis chip⁽⁶⁹⁾. The chip has gel wells and microchannels fabricated in glass to interconnect these wells. Using an Agilent High Sensitivity DNA kit (Agilent Technologies), all wells were filled with gel dye, and appropriate wells with either DNA marker (internal upper and lower marker), ladder or sample⁽⁶⁹⁾. In each run, the Bioanalyser can run 12 samples in 30 minutes on a disposable chip. In addition to 12 sample wells, the chip has four further wells used for the molecular weight ladder of known fragment sizes (supplied in the kit)⁽⁷⁰⁾. The samples were loaded (according to the manufacturer's guide) on the DNA 7500 LabChips. Briefly, nine μ L of gel dye mix was added into the appropriate well⁽⁷⁰⁾. The gel-dye mixture was forced into the microchannel by using a 1 mL syringe. This was followed by adding 5 μ L of the upper and lower marker in each sample well, 1 μ L of molecular weight ladder in the appropriate well, and 1 μ L of samples in the sample well⁽⁷⁰⁾. The chip was vortexed for one minute, immediately inserted into the bioanalyser, and processed for 30 minutes⁽⁷⁰⁾.

The chip is integrated with an electrical circuit, and fragments are separated electrophoretically by size on the chip, where the smaller DNA fragments migrate faster than the larger fragments⁽⁶⁹⁾. A fluorescent dye binds to DNA, and a laser detects the fluorescence, and the data is displayed as both traditional gel images and as electropherograms⁽⁶⁹⁾. The upper and lower markers are used as internal standards that align the ladder data with DNA sample data⁽⁶⁹⁾. The two markers bracket the overall sizing range of the DNA⁽⁶⁹⁾. Thus, they are internal standards aligning the ladder data (Figure 10) from the sample wells⁽⁶⁹⁾.

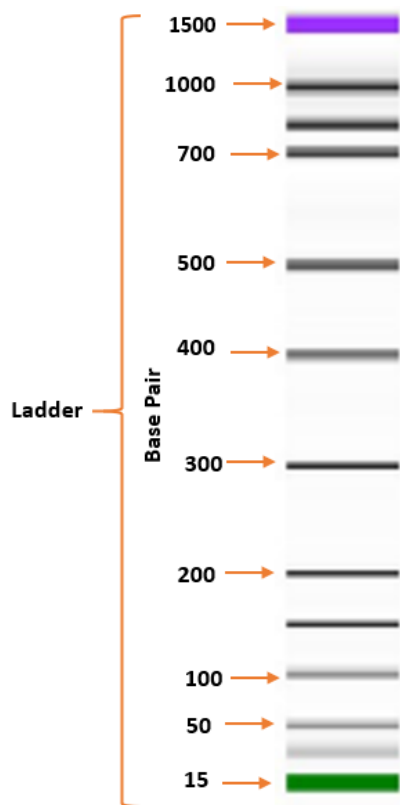


Figure 10: Example output from Agilent 2100 Bioanalyser Electrophoresis. The ladder shows the migration of 13 fragments of known size through the gel. The green band indicates the lower marker, while the purple band indicates the upper marker.

It is necessary to run the lower and upper markers to compensate for the drift effects arising during the chip electrophoresis⁽⁶⁹⁾. Drift effects are sometimes caused by differences in the sample wells running conditions such as current strength, sample contamination and sample concentration; therefore, the marker aligns the DNA sizes so they can be compared.

2.2 Preparation of Biotinylated DNA Fragments

BioNick™ Labeling System kit (Thermo Fisher Scientific, Invitrogen™) was utilised to biotinylate the fragmented DNA. In this kit, the biotin labels the DNA by nick translation. The DNase I present in the reagent mix randomly nicks the DNA at low enzyme concentrations in the presence of magnesium chloride⁽⁷¹⁾. Using the 3'-OH terminals of the nick as a primer, DNA Polymerase I synthesises DNA complementary to the strand, which has not been nicked in a 5'-3' direction. At low temperature, the DNA Polymerase I replaces the removed nucleotides with deoxyribonucleoside triphosphates (dNTP); thus, the unlabeled DNA in the reaction is replaced with newly synthesised biotin labelled DNA⁽⁷¹⁾ with biotin inserted approximately every 20th nucleotide⁽⁶⁵⁾.

The 300bp fragment was selected for biotinylation. All the reagents (10 × dNTP Mix, 10 X Enzyme Mix, Control DNA, Stop Buffer, Distilled Water) used for this method were supplied in the kit. The steps of the biotinylation are as follows⁽⁶⁵⁾:

In a micro-centrifuge tube placed on ice, the following volumes were added to reach a total volume of 45 µL, as shown in Table 3 below.

Table 3: Volumes for DNA biotinylation.

	Fragmented DNA (µL)
10× dNTP Mix	5
DNA (1 µg)	11.3 (at 88.4 ng/µL)
Distilled water	23.7
10× enzyme mix	5

The tubes were well mixed and centrifuged at 3000 g for one minute. The tubes were then incubated at 16°C for one hour in a refrigerated water bath (Life Technologies, Julabo F18). After incubation, the tubes were removed from the water bath, placed on ice, and 5 µL of stop buffer was added to stop the reaction. Next, the unincorporated nucleotides were removed through ethanol precipitation by adding 5 µL of 3M sodium acetate and 100 µL of absolute cold ethanol to the reaction mix. The tubes were well mixed and placed at -70°C for 15 minutes, after which both Eppendorf tubes were spun in a cooling centrifuge (Eppendorf centrifuge 5424 R) at 15,000 g for 10 minutes at 4°C. The supernatant was removed by tilting the tubes on the side opposite to where the DNA was likely to accumulate. The white strand of DNA was left to air dry for 20 minutes. Then, the DNA was resuspended in 50 µL of sterile water. The ethanol precipitation stage was repeated, and the biotinylated DNA was resuspended in TE buffer and stored at

either 4°C or -20°C depending on the usage time. DNA stored at 4°C was used in further experiments within 48 hours, whereas -20°C was used for longer storage times⁽⁶⁰⁾.

The last step of the kit method was later modified: red cell preservative solution (*BIO-RAD* Cell Stab) was used to resuspend biotinylated DNA in place of TE buffer, as the DNA would later be added to red blood cells.

2.2.1 Detection of Biotinylation of DNA

To assess the success of the biotinylation of DNA, traditional gel electrophoresis was performed. This method was utilised based on the principle that the addition of biotin and streptavidin to DNA would slow the DNA migration down during electrophoresis, producing a shift of DNA distribution when compared to the non-biotinylated DNA⁽⁷²⁾. However, the samples failed to be detected in gel electrophoresis. Therefore, as the gel electrophoresis could not show biotinylation of DNA, and since the biotinylated DNA sample was limited in quantity, it was decided to use a streptavidin detection method.

Streptavidin has a molecular weight of 55,000 Daltons and is a protein purified from the bacteria *Streptomyces avidinii*. It has a high affinity to biotin and binds four biotin molecules per molecule of streptavidin⁽⁷³⁾. Thus, it can be used as a bridging method to link a biotinylated probe to a biotinylated enzyme⁽⁷³⁾ or, in this case, biotinylated DNA to FSL biotin on kodeocytes. For this research, it was uncertain how much streptavidin would be optimal for detecting the success of biotinylation, therefore different concentrations of streptavidin ranging from 0.83 mg/mL-2.5 mg/mL were used to assess the success of biotinylating DNA.

During method development, it was necessary to avoid wastage of precious and limited biotinylated DNA sample. In early proof of concept here, it was decided to use a surrogate for biotinylated DNA with similar properties to DNA⁽⁷⁴⁾.

Atri-PAA-biotin was selected as a surrogate for biotinylated DNA. Atri-PAA-Biotin (GlycoNZ) is a man-made blood group A trisaccharide antigen coupled with polyacrylamide spacer and biotin (Figure 11). It is a 20 kDa glycopolymer with a similar molecular weight to DNA⁽⁷⁵⁾. Like the biotinylated DNA sample, it includes biotin. The fact that it also expresses blood group A antigen proved useful in later experiments, where binding to an anti-A antibody could be utilised as a detection method.

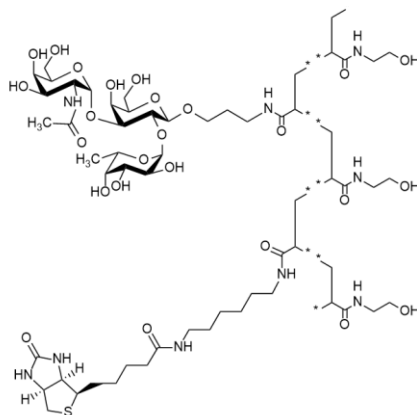


Figure 11: Atri-PAA-Biotin construct. It comprises blood group A trisaccharide antigens, polyacrylamide spacer and biotin.

Atri-PAA-Biotin has approximately ten biotins in a single molecule. This provided information about the concentration of streptavidin added that would be in excess for the binding between biotin and streptavidin ⁽⁷⁵⁾. Biotin and streptavidin have a high affinity, and previous work has shown that one biotin residue in Atri-PAA-Biotin is sufficient for binding⁽⁷⁵⁾.

2.2.2 Analysis of Biotinylated Polymer (Atri-PAA-Biotin) via Streptavidin-coated Plate

The streptavidin detection method was based on the binding of biotin to a streptavidin-coated plate. Atri-PAA-Biotin and streptavidin binding were analysed on a modified sandwich Enzyme-Linked Immunosorbent Assay (ELISA) on a streptavidin-coated polystyrene plate (ThermoFisher Scientific).

Two detection methods were assessed by ELISA, one with a colour signal and one with fluorescence (Figure 12 and Figure 13), to evaluate Atri-PAA-Biotin and streptavidin-coated plate binding success. Varying concentrations of both Atri-PAA-Biotin and enzyme labelled streptavidin were prepared to determine the minimum concentration which the streptavidin-coated plate could detect.

The first detection method used the colourimetric method, utilising the principle that the colour of the substrate para-nitrophenylphosphate (PNPP) changes colour from clear to yellow when chemically altered by a compatible enzyme (for example, alkaline phosphatase). The method is summarised in Figure 12.

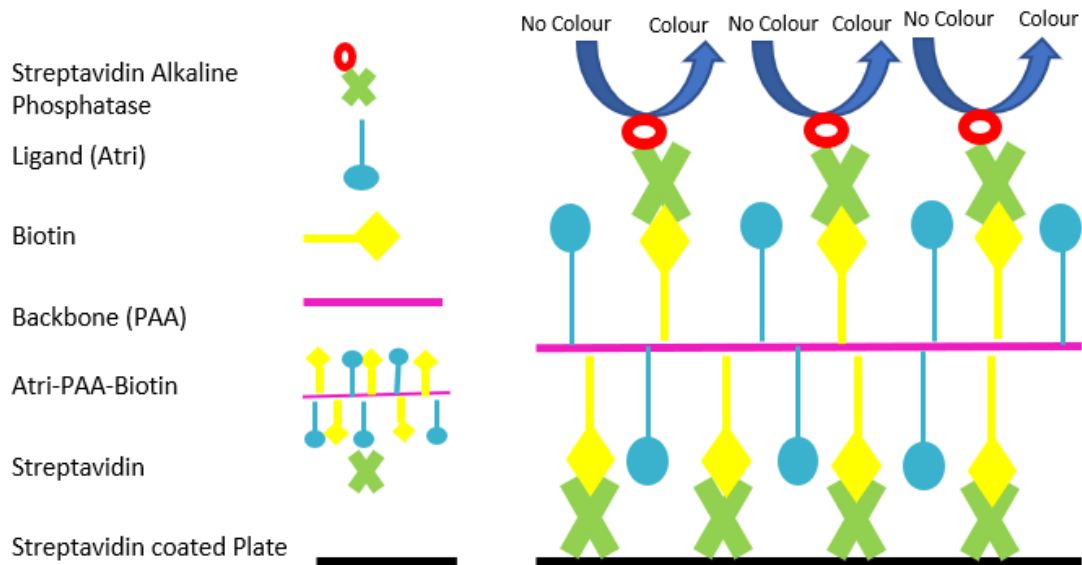


Figure 12: Modified sandwich Enzyme-Linked Immunosorbent Assay (ELISA) format to detect varying concentrations of biotinylated samples (Atri-PAA-Biotin) bound to a streptavidin-coated plate. Biotinylated samples bind to streptavidin on the plate. Washing removes unbound material. Streptavidin alkaline phosphatase (AP) enzyme binds to bound biotin in the biotinylated sample. Alkaline phosphatase converts the substrate PNPP to a yellow product with maximal absorbance at 405nm.

Atri-PAA-Biotin was prepared in varying concentrations (10 $\mu\text{g/mL}$, 1 $\mu\text{g/mL}$, 0.1 $\mu\text{g/mL}$, 0.01 $\mu\text{g/mL}$, 0.001 $\mu\text{g/mL}$). The binding of these varying concentrations of Atri-PAA-Biotin to streptavidin-coated plates was detected by the method shown in Figure 12. The method was as follows, with all tests performed in duplicates.

The streptavidin-coated plate was washed four times with 200 μL of 2% BSA/TBS to prevent non-specific binding. To separate wells, 100 μL of PBS or Atri-PAA-Biotin at 10, 1, 0.1, 0.01 and 0.001 $\mu\text{g/mL}$ were added.

The plates were incubated at room temperature for two hours. After incubation, the plate was washed four times with 200 μL of 2% BSA/TBS to remove the unbound material. Streptavidin Alkaline Phosphatase at a final concentration of 150 mM (ThermoFisher) was added (100 μL) to all wells. The plate was then incubated at room temperature for 30 minutes. After incubation, the plate was washed three times with 200 μL of 2% BSA/TBS and one time with 200 μL of substrate buffer. After washing, 100 μL of PNPP (ThermoFisher) was added to all the wells, and the plate was incubated at room temperature for 30 minutes. After incubation, the plate was read in a plate reader (Tecan Spark 10m) at 405nm.

A second detection method with fluorescent signal utilising Alexa Fluor 488 was performed. The summary of the method is shown in Figure 13.

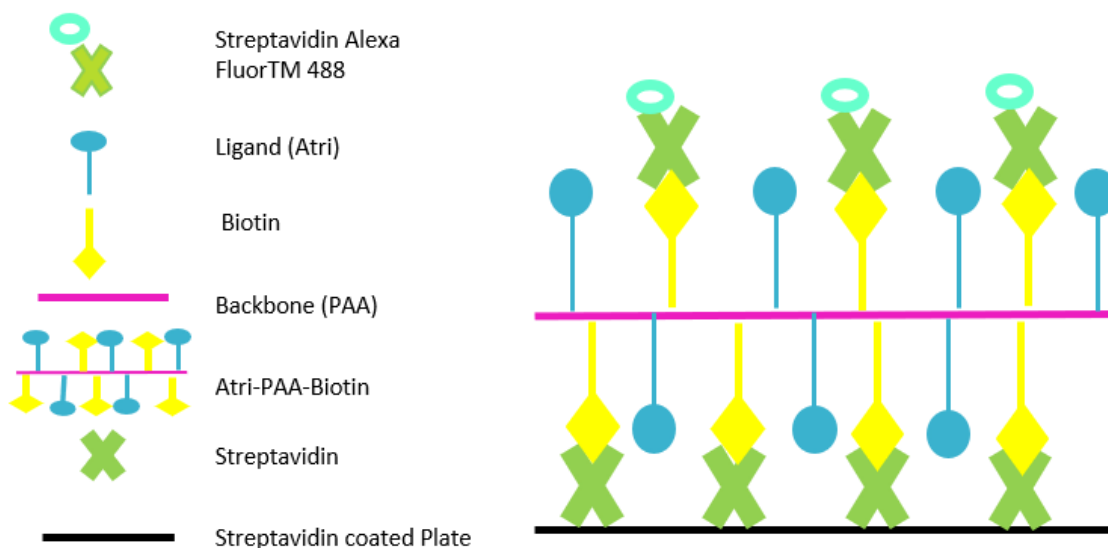


Figure 13: Modified ELISA format to detect varying concentrations of biotinylated samples bound to the streptavidin-coated plate. Biotinylated samples bind to streptavidin on the plate. Washing removes unbound material. Streptavidin Alexa Fluor™ 488 binds to bound biotin in the biotinylated samples. The fluorescence intensity of Alexa Fluor™ 488 is measured in a plate reader.

The method was as follows:

The streptavidin-coated plate was washed four times with 200 μL of 2% BSA/TBS, and all tests were performed in duplicates. To each well, 100 μL of PBS, Atri-PAA-Biotin (10 $\mu\text{g}/\text{mL}$) (without Streptavidin Alexa Fluor™ 488), Atri-PAA-Biotin at 10, 1, 0.1, 0.01 and 0.001 $\mu\text{g}/\text{mL}$ were added.

The plates were incubated at room temperature for 2 hours. After incubation, the plate was washed four times with 200 μL of 1x PBS. Streptavidin Alexa Fluor™ 488 at a concentration of 10 $\mu\text{g}/\text{mL}$ (ThermoFisher) was added in a volume of 100 μL to all wells except the second well only had Atri-PAA-Biotin. The plate was then incubated at room temperature for 30 minutes. After incubation, the plate was washed four times with 200 μL of 1x PBS. After washing, the fluorescence intensity was read in a plate reader (Tecan Spark 10m) at an excitation wavelength of 492 nm and an emission wavelength of 520 nm.

Both colourimetric and fluorescent methods proved that biotinylated polymer could bind to streptavidin, but the colourimetric method showed less “background noise” in comparison to the fluorescent method, and colourimetric was used moving forward.

The next step was to determine a minimum concentration of biotinylated polymer that could be used in this method (again, using the surrogate for biotinylated DNA). In the previous method, concentrations of Atri-PAA-Biotin were tenfold in comparison to each other. In order to test method sensitivity at twofold rather

than tenfold concentrations, a doubling dilution of Atri-PAA-Biotin was performed to determine the minimum concentration, with a starting concentration of 10 µg/mL.

The doubling dilution of 10 µg/mL of Atri-PAA-Biotin was performed as per Figure 14.

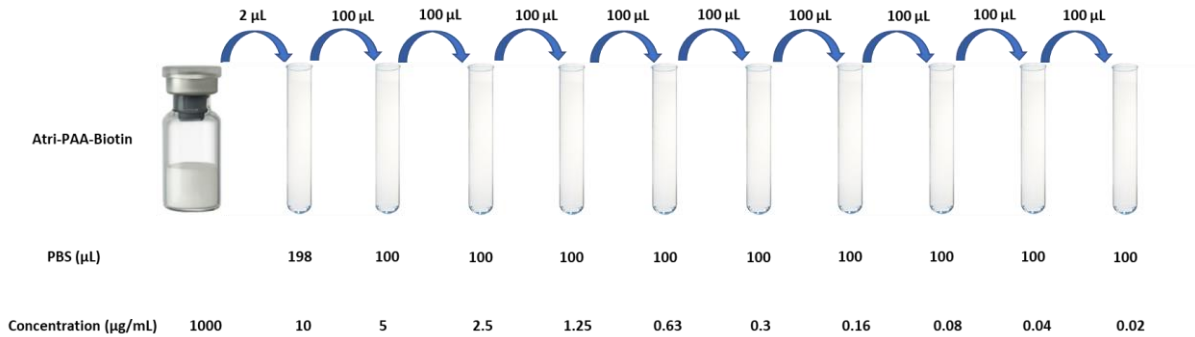


Figure 14: Doubling dilutions of Atri-PAA-Biotin and biotinylated DNA. 10 µg/mL of Atri-PAA-biotin was prepared from the stock by adding 2 µL of Atri-PAA-biotin to 198 µL of PBS, and a doubling dilution was performed till 0.02 µg/mL of concentration was achieved

The streptavidin-coated plate was developed, as described above in Figure 12. This established that the colourimetric method was suitable to detect the biotinylated polymer down to concentrations of 0.02 µg/mL. It was now appropriate to re-introduce the biotinylated DNA sample in place of the surrogate Atri-PAA-Biotin.

Accordingly, a doubling dilution of 300bp biotinylated DNA was prepared, as shown in Figure 15.

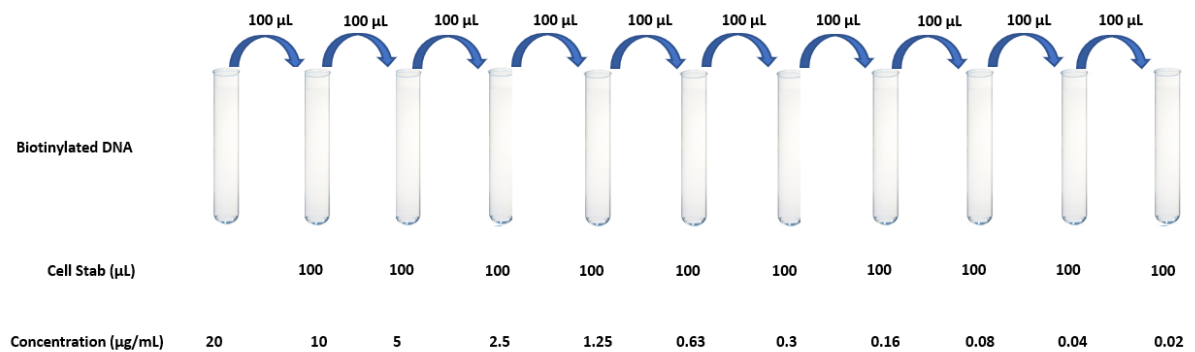


Figure 15: Doubling dilutions of biotinylated DNA. 10 µg/mL of biotinylated DNA was prepared by adding 100 µL of 20 µg/mL of biotinylated DNA to 100 µL of PBS, and a doubling dilution was performed till 0.02 µg/mL of concentration was achieved.

The streptavidin-coated plate was developed as described above.

2.3 Preparation of Biotin-Streptavidin Kodecytes

FSL-biotin (Kode Biotech Materials Limited) was reconstituted by adding one mL of PBS to 0.5 mg of FSL freeze-dried powder to prepare a solution at 0.5 mg/ mL (240.5 $\mu\text{Mol/L}$). The suspension was vortexed for one minute and left at room temperature to rest for 30 minutes. FSL-biotin was diluted to 20 $\mu\text{Mol/L}$ in PBS, with a final volume of 200 μL .

In a test tube, 200 μL of 20 $\mu\text{Mol/L}$ FSL-biotin and 200 μL of washed group O packed RBC (PRC) were added. In another test tube, 100 μL of PBS and 100 μL of blood group O PRC were added (process control). The tubes were incubated for two hours at 37°C with gentle mixing at the one-hour interval. Following incubation, the kodecytes were suspended to 5% in Cell Stab (*Bio-Rad*, Cat #: 005650) and left overnight at 4°C. No washing of kodecytes was required⁽⁷⁶⁾.

2.3.1 Preparation of Streptavidin Kodecytes

FSL-Biotin kodecytes were secondarily modified noncovalently with streptavidin by incubating FSL-Biotin kodecytes with streptavidin in excess⁽⁴⁹⁾. FSL-Biotin kodecytes loaded with streptavidin will be referred to as streptavidin kodecytes from here onwards.

Biotin kodecytes and un-koded process control tubes were centrifuged to sediment the cells, and the supernatant was discarded. Then, the biotin kodecytes and the process control cells were washed three times with PBS. Following washing, streptavidin kodecytes and controls were prepared, as shown in Table 4.

Table 4: Preparation of kodecytes and controls. Tube 1 was un-koded cells with streptavidin (a control checking for non-specific binding of streptavidin. Tube 2 had biotin kodecytes with no streptavidin (control), while tubes 3 and 4 were duplicate tests and had biotin kodecytes and streptavidin. All tubes were incubated at room temperature for 30 minutes.

	Tube 1 (control)	Tube 2 (control)	Tube 3	Tube 4
Biotin Kodecytes	× (O cells)	✓	✓	✓
PBS	✓	✓	✓	✓
Streptavidin	✓	× (PBS)	✓	✓

2.3.2 Analysis of Ability of Streptavidin Kodecytes to Capture Biotinylated Polymer

A proof-of-concept experiment was designed to prove that streptavidin can be used as a bridge to link a biotin polymer to biotin kodecytes. Atri-PAA-Biotin was again used as a surrogate model here.

The concept of joining Atri-PAA-Biotin to biotin kodecytes via streptavidin bridge was assessed using an agglutination assay, and the concept is depicted in Figure 16.

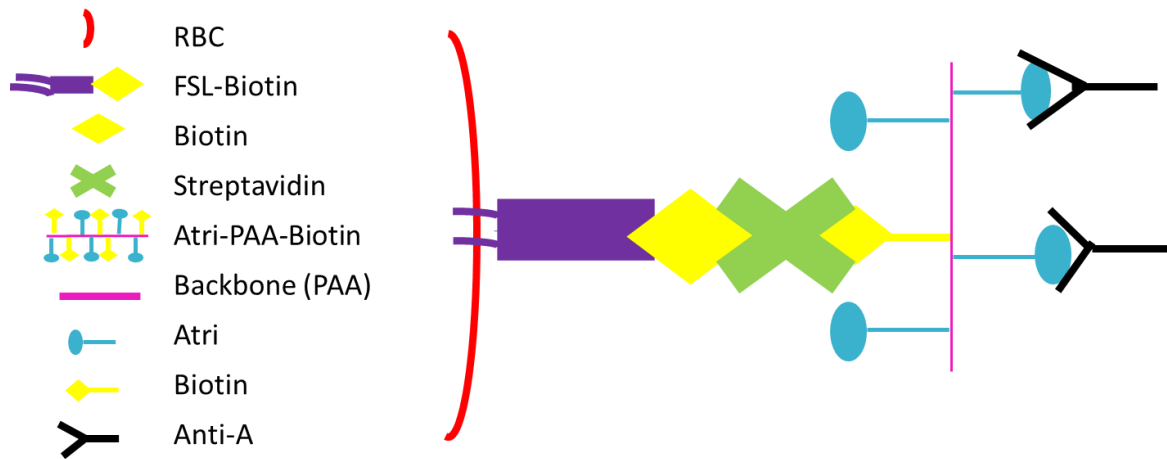


Figure 16: Kodecyte with Atri-PAA-Biotin polymer. This model was prepared by attaching Atri-PAA-Biotin to streptavidin kodecytes. Detection was possible by reacting the streptavidin kodecytes-Atri-PAA-Biotin complex with Anti A.

Monoclonal IgM Anti A has specificity for blood group A trisaccharide on the Atri-PAA-Biotin and results in agglutination⁽⁷⁷⁾ when linked to red cells, as shown in Figure 16. Column agglutination technology (CAT) was selected as the platform for detecting agglutination in a saline technique. Neutral gel cards (*BIO-RAD* NaCl, Enzyme Treatment and Cold Agglutinins) were used. In this card, the gel in the column has particles of a specific size, allowing agglutinated cells to be trapped (Figure 17 A) in the gel and non-agglutinated red blood cells to pass through to the bottom (Figure 17 B) of the column⁽⁷⁸⁾.

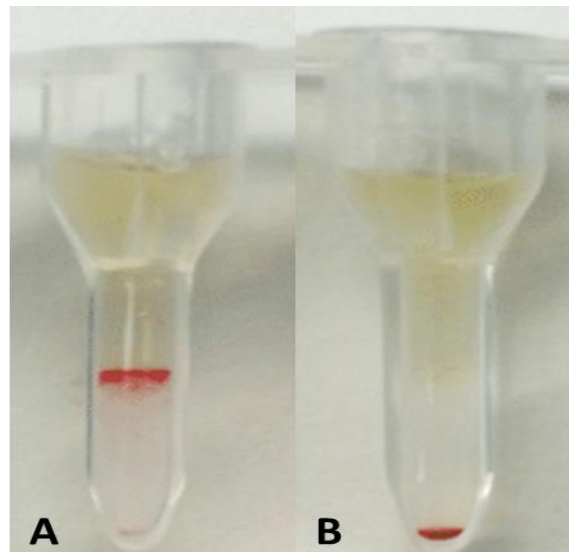


Figure 17: Column agglutination technology using neutral gel cards in saline. Image A shows agglutinated cells trapped in the gel, while image labelled B shows non-agglutinated cells settled at the bottom of tubes. Image reproduced with permission⁽⁷⁹⁾.

The method was as follows:

Streptavidin kodecytes and appropriate controls were spun to sediment the cells, and the supernatant was discarded. All tubes were washed three times in PBS. After washing, fresh PBS was added to all tubes to prepare a 5% suspension of cells. To tubes 1, 2 and 4 (Table 5), 500 μ L of 10 μ M Atri-PAA-Biotin and tube 3, 500 μ L of PBS, was added. All tubes were incubated at room temperature for 40 minutes. Following incubation, the tubes were spun at high speed for one minute, and the supernatant was discarded. This was followed by washing all tubes three times with 1 mL of 1 \times PBS. After washing, 1% cell suspensions were prepared in PBS. In a gel card (*BIO-RAD*), 50 μ L of Anti-A and 50 μ L of 1% suspension was added (Table 5). The gel card (NaCl, Enzyme Treatment and Cold Agglutinins) was spun (*BIO-RAD* ID-Centrifuge 12 S II) for 10 minutes and checked for agglutination.

Table 5: Preparation of streptavidin kodecytes Atri-PAA-Biotin -Anti-A complexes. Tube 1 is a control with no biotin kodecytes; tube 2 a control with no streptavidin; tube 3 a control with no Atri-PAA-Biotin, and tube 4 is all the polymers, kodecytes and antigens for streptavidin to create a bridge and agglutinate with Anti-A.

	Tube 1 (control)	Tube 2 (control)	Tube 3 (control)	Tube 4
Biotin kodecytes (20 μ Mol)	\times (PBS)	✓	✓	✓
Streptavidin (7.5 μ Mol)	✓	\times (PBS)	✓	✓
Atri-PAA-Biotin (10 μ Mol)	✓	✓	\times (PBS)	✓
Anti-A	✓	✓	✓	✓

It was expected that only cells in tube 4 (Table 5) should agglutinate, as this is the only tube where all elements of the reaction are present.

2.4 Preparation of Biotin-Streptavidin- Biotinylated DNA Kodecytes and Evaluation of Reticulocyte Mimic

Following on from the surrogate assays, biotinylated DNA samples were prepared and used with streptavidin kodecytes to prepare mimic reticulocytes. Volumes and concentrations were guided by results from the successful experiments with Atri-PAA-Biotin.

Biotin kodecytes were prepared as per method 2.3. Biotin kodecytes were loaded with streptavidin as per method 2.3.1 to make streptavidin kodecytes. Biotinylated DNA (300bp fragments) at a concentration of 10 ng/mL was added to streptavidin kodecytes and incubated at room temperature for ten minutes.

2.5.1 Analysis of Mimic Reticulocytes by Aggregation

The success of the preparation of mimic reticulocytes was assessed via aggregation. It was not possible to use the agglutination method with Anti-A described in section 2.3.2 with mimic reticulocytes as mimic reticulocytes do not include A antigen. However, mimic reticulocytes should aggregate as it is hypothesised that streptavidin would form a bridge between the biotin kodecytes and biotinylated 300bp DNA and form aggregates.

Aggregation was assessed by briefly centrifuging mimic reticulocytes and appropriate controls to sediment and then transferring cells to wells of a CAT neutral gel card (*BIO-RAD* NaCl, Enzyme Treatment and Cold Agglutinins). This was based on the principle that aggregates would be trapped in the gel.

2.5.2 Analysis of Mimic Reticulocytes by Haematology Analyser

Based on the principles of reticulocytes detection by haematology analysers presented in the introduction, mimic reticulocytes were analysed in the Sysmex (XN-20) analyser.

Biotin kodecytes were prepared with FSL-biotin at 20 μ Mol as per method 2.3. After resting the FSL-Biotin kodecytes overnight at 4°C, the cells were briefly centrifuged to sediment cells, and the supernatant was removed. Nine different tubes were prepared (Table 6), a series of mimic reticulocytes prepared with two different concentrations of biotinylated DNA and controls (normal blood). All tubes were incubated at room temperature for ten minutes.

Table 6: Sample preparation for mimic reticulocytes asses via Sysmex analyser. Two concentrations (20 µg/mL and 10 µg/mL) of 300bp biotinylated DNA were prepared and assessed via the haematology analyser. Tubes 1-3 had 20 µg/mL of 300bp biotinylated DNA, tubes 4-6 had 10 µg/mL of 300bp biotinylated DNA and tubes 7-9 were controls. Tube 1 had the biotin kodecytes, 20 µg/mL 300bp biotinylated DNA and streptavidin as the bridge. In contrast, tubes 2 and 3 had no streptavidin to form a bridge and no biotin kodecytes for streptavidin to bind to, respectively. Tube 4 had the biotin kodecytes, 20 µg/mL 300bp biotinylated DNA and streptavidin as the bridge. In contrast, tubes 5 and 6 had no streptavidin to form a bridge and no biotin kodecytes for streptavidin to bind to, respectively. Tube 7 had no streptavidin and 300bp biotinylated DNA, and tube 8 had no biotinylated DNA. Tube 9 had un-koded cells (O washed, packed cells) with no streptavidin and biotinylated DNA.

	Samples								
	20 µg/mL			10 µg/mL			Controls		
	Biotinylated DNA			Biotinylated DNA					
	Tube	Tube	Tube	Tube	Tube	Tube	Tube	Tube	Tube
	1	2	3	4	5	6	7	8	9
Biotin kodecytes (20 µMol)	✓	✓	×	✓	✓	×	✓	✓	×
Streptavidin (7.5 µMol)	✓	×	✓	✓	×	✓	×	✓	×
300bp Biotinylated-DNA	✓	✓	✓	✓	✓	✓	×	×	×

For final preparation for analysis in the haematology analyser, a mixture was prepared, consisting of 5% of mimic reticulocytes and 95% O cells (the same cells used to prepare the kodecytes). The mixture was chosen to mimic natural reticulocyte percentages present in the patients with somewhat raised reticulocytes counts⁽⁸⁾. The mixtures were diluted from the packed cells to a 50% suspension in CellStab, to mimic a haematocrit representative of a normal adult blood sample⁽⁸⁾.

Samples were analysed in a Sysmex (XN-20) analyser by standard protocols⁽⁶⁾.

2.5.3 Analysis of Mimic Reticulocyte by Supravital Staining

Mimic reticulocytes were also analysed via supravital staining. Brilliant Cresyl Blue (BCB) was used to visualise and enumerate reticulocytes. The BCB stains the reticular filaments of nucleic acid precipitated in immature red blood cells.

Two volumes of samples and controls (Table 6) were added to one volume of filtered BCB stain in separate tubes. The tubes were incubated at 37°C for two hours. The mixture was resuspended, and a conventional thin smear⁽⁸⁾ was prepared and left to air dry for five minutes. The smears were prepared in duplicates. All smears were then examined under a 50x and 100x oil immersion lens using a light microscope (Olympus).

3 Results

3.1 DNA Preparation and Fragmentation

Plant DNA extraction using buffers prepared ‘in-house’

As stated in the method section 2.1.1, two different buffers were prepared and used to extract DNA, and the purity and concentrations of extracted DNA were compared. Figure 18 shows a visual representation of the DNA extraction using Extraction (A-C) and Edwards buffer (D-F) with tomato leaves.

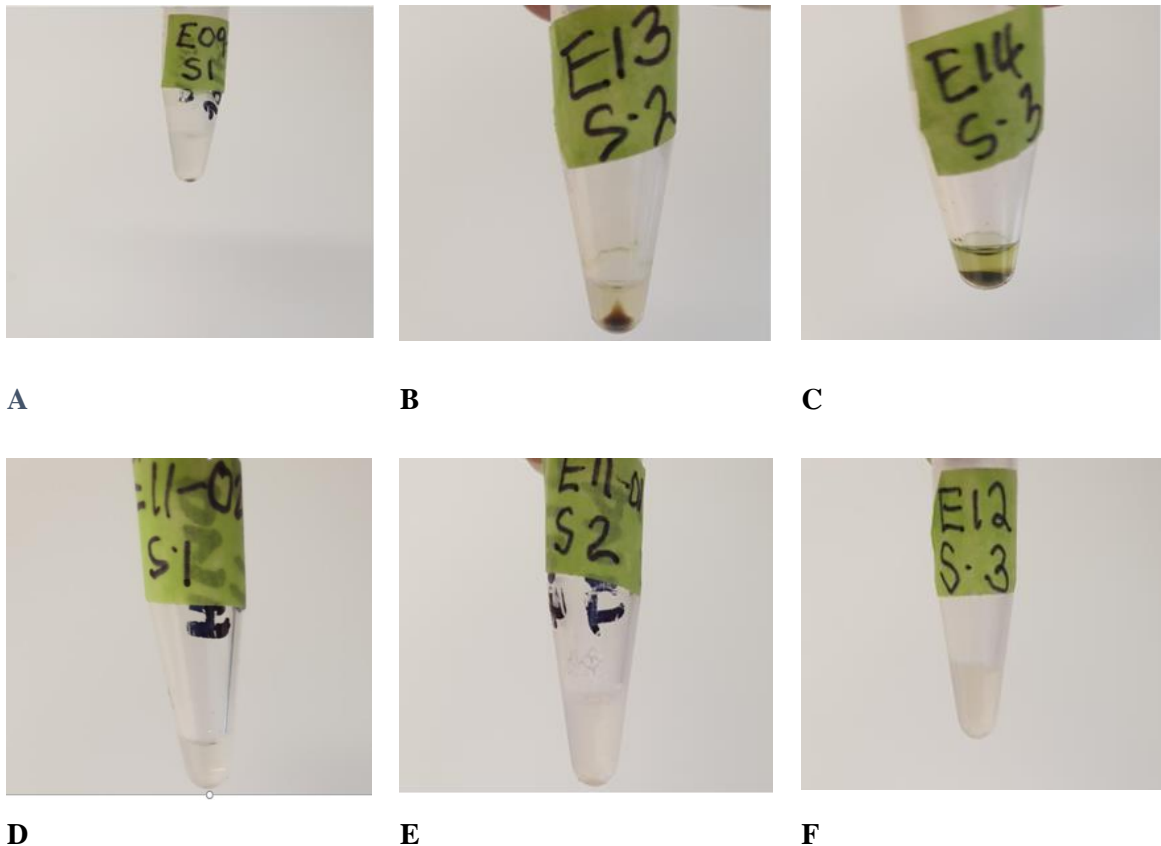


Figure 18: Comparison of DNA pellet of Extraction buffer and Edwards's buffer. Image A-C shows DNA extracted using an Extraction buffer with green pellets indicating plant debris contamination, and images D-F images show extracted DNA using Edwards's buffer with transparent, less contaminated pellets.

The visual representation in Figure 18, images A-C shows DNA extraction with Extraction buffer and reveals green residue at the tubes bottom. Images D-F show DNA extraction with Edwards buffer, which has a clear residue at the tubes bottom. In contrast to the Extraction buffer, the clear pellets observed with Edwards buffer indicate relatively clean DNA.

Table 7: DNA extraction results from tomato leaves using Extraction buffer. The results show DNA purity and concentration measured by spectrophotometry (NanoVue). Samples A-C represent multiple extractions of different aliquots of a single DNA sample of tomato leaves.

Samples	Extraction Buffer	
	Average A_{260}/A_{280} Ratio	Average DNA Concentration (ng/ μ L)
A	1.6	34
B	2	117
C	2.3	179

Purity values ranged from 1.6-2.3 (optimal range: 1.7-2.0). A ratio below 1.7 indicates the sample is contaminated with protein, and a ratio above 2.0 suggests RNA contamination⁽⁸⁰⁾. The results showed a consistent average DNA purity ranging from 1.5-1.7 (optimal range: 1.7-2.0). However, there is still some protein contamination evident, with ratios less than 1.7⁽⁸⁰⁾.

Table 8: DNA extraction results from tomato leaves using Edwards buffer. The results show DNA purity and concentration measured by spectrophotometry (NanoVue). Samples D-F represent multiple extractions of different aliquots of a single DNA sample of tomato leaves.

Samples	Edwards Buffer	
	Average A_{260}/A_{280} Ratio	Average DNA Concentration (ng/ μ L)
D	1.5	22
E	1.7	160
F	1.6	90

The visual representation is consistent with the values obtained from the average purity values (Table 7), and this is consistent with the values obtained from the average purity shown in Table 8.

DNA was also extracted from spinach leaves with Edwards buffer, and the results are shown in Table 9. As the DNA pellets in sample 1 and 2 did not dissolve, the DNA purity and concentration results were measured from the supernatant.

Table 9: DNA extraction results (spinach leaves in Edwards buffer). The results show DNA purity and concentration from the sample supernatant, measured by spectrophotometry (NanoVue). Sample 1 and 2 represent different aliquots of single DNA extraction from spinach leaves

Samples	A ₂₆₀ /A ₂₈₀ ratio	DNA Concentration (ng/ μL)
1	2	320
2	2	376

The results show a high DNA concentration and relatively pure extraction. However, the DNA pellet was still partially intact, indicating contamination⁽⁸⁰⁾.

Another DNA extraction was performed using baby spinach leaves. After the DNA pellet was left in sterile water to dissolve overnight, the purity and concentration were measured the following day. The results in Table 10 are from supernatant as again the pellet did not completely dissolve.

Table 10: DNA extraction results of undissolved DNA (spinach leaves in Edwards Buffer). The results show DNA purity and concentration from the supernatant measured by spectrophotometry (NanoVue). Sample 1 to 6 represent different aliquots of a single DNA extraction from spinach leaves

Samples	A ₂₆₀ /A ₂₈₀ ratio	DNA Concentration (ng/ μL)
1	2.1	64
2	2.0	68
3	2.1	72
4	2.1	56
5	2.0	71
6	2.0	81

The DNA pellets of sample 1-6 (Table 10) did not dissolve even after leaving them overnight. These results indicate that the DNA extraction is not pure as the A₂₆₀/A₂₈₀ ratio is greater than 2.0⁽⁸⁰⁾. The DNA concentration was relatively constant across the six extractions but probably falsely low due to the undissolved DNA being unavailable for measurement.

All the other optimisations steps performed to dissolve the DNA pellet, as mentioned in Methods, were unsuccessful in dissolving the pellet, and the DNA was regarded as contaminated.

DNA Extraction using Plant Extraction DNA Kit

The kit with tomato leaves stored for four weeks at 4 °C is shown in Table 11.

Table 11: DNA extraction results (stored tomato leaves) with PureLink® Plant Total DNA Purification Kit. The results show DNA purity measured by NanoVue and concentration by fluorometry (Qubit).

	NanoVue	Fluorometer
DNA	A_{260}/A_{280} ratio	DNA Concentration (ng/ μ L)
	1.7	0.4

Although the DNA was relatively pure (A_{260}/A_{280} ratio = 1.7), there was a very low yield. The low concentration was likely due to old leaves, which contains phenol which oxidises the DNA irreversibly⁽⁵⁷⁾.

Fresh baby spinach leaves were used for the subsequent extraction, and the DNA purity and concentration were measured using a fluorometer, as shown in Table 12.

Table 12: DNA extraction results using the kit. The results show DNA concentration measured by a fluorometer (Qubit). Sample 1 to 4 represents different aliquots of a single DNA extraction from spinach leaves.

Samples	DNA Concentration (ng/ μ L)
1	21
2	24
3	14
4	14

The results presented in Table 12 show relatively consistent DNA concentration across four samples. Compared to Table 11, DNA was extracted from old tomato leaves, the DNA concentration is higher when extracted from fresh spinach leaves but still too low for downstream application. Samples 1 and 2 were retained for fragmentation, and another DNA extraction was performed to extract more DNA using fresh spinach leaves. The results are shown in Table 13.

Table 13: DNA extraction results from spinach leaves using the kit. Sample 1 to 6 represents different aliquots of a single DNA extracted from spinach leaves. The results show DNA concentration measured by spectrophotometry (NanoVue) and fluorometer (Qubit).

Samples	Spectrophotometer		Fluorometer
	A_{260}/A_{280} ratio	DNA Concentration (ng/ μ L)	DNA Concentration (ng/ μ L)
1	1.8	13	9
2	1.8	14	
3	1.7	16	
4	1.8	12	
5	1.7	14	
6	1.8	12	10

The results show pure DNA extraction with an average of 1.8 ratio but consistently low DNA concentration with the highest concentration of 16 ng/ μ L and the lowest concentration of 12 ng/ μ L. The substitution of stored for fresh leaves had not resolved the consistently insufficient DNA yields.

DNA extraction Using Human Buffy Coat

Using a human buffy coat to extract DNA, somewhat higher DNA concentrations and consistently satisfactorily A_{260}/A_{280} ratios of DNA were achieved.

The purity and DNA concentration of DNA extracted from the human buffy coat was measured using the NanoVue, as shown in Table 14.

Table 14: DNA extraction results from the human buffy coat by proteinase K method. The results show DNA purity and concentration measured by spectrophotometry (NanoVue) and fluorometry (Qubit). Samples 38A-38E represent different aliquots of a single buffy coat.

Samples	A_{260}/A_{280} ratio	DNA Concentration (ng/ μ L)
38 A	1.9	368
38 B	2.0	125
38 C	1.9	308
38 D	1.9	413
38 E	1.9	155

Six aliquots (38 A -38 E) of genomic DNA extracted from human blood yielded higher DNA concentrations than those from other methods. Sample 38 D had the highest concentration of DNA 413 ng/ μ L followed by sample 38 A 368 ng/ μ L while 38 E and 38 B had the lowest concentration of 155 ng/ μ L and 125 ng/ μ L, respectively. The average A_{260}/A_{280} ratio was 1.9, which indicated consistently pure DNA. It was also technically easier to scale this method up to extract more DNA. Therefore, extraction of human genomic DNA from buffy coat using the proteinase K method became the preferred method for this project's downstream applications.

3.1.1 DNA Fragmentation and Analysis- Human Buffy Coat

Selected DNA samples extracted from human buffy coat were subjected to DNA fragmentation. Sample 38 D (Table 14) DNA was fragmented using 300bp protocol, while E38 E (Table 14) was fragmented using the 500bp protocol. Sample 38 B (Table 14) was also fragmented using the needle shearing technique described in 2.1.3 b Needle Shearing.

All DNA samples were diluted to 10 ng/ μ L (Table 15) using the concentration values from Qubit 2.0 fluorometer before analysing in the Bioanalyser⁽⁸¹⁾. The empty regions in the table indicate those samples did not require any further dilution as they met the required concentration. The highlighted cells indicate the final DNA concentrations.

Table 15: Dilutions of unfragmented and fragmented DNA for Agilent 2100 Bioanalyser High Sensitivity DNA Kit assay. The empty regions in the table indicate those samples did not require any further dilution as they met the required concentrations. The numbers in the boxes indicate the final DNA concentrations.

Samples	First Dilution			Second Dilution			Third Dilution		
	Water μ L	DNA μ L	Fluorometer ng/ μ L	Water μ L	DNA μ L	Fluorometer ng/ μ L	Water μ L	DNA μ L	Fluorometer ng/ μ L
38 B Needle Shearing	4	1	>60	9	1	8			
38 E Covirus-500bp	3.83	1	15	1.7	3.3	12.	9	1	2
38 E Unfragmented DNA	4.1	1	>60	9	1	19	9	1	1
38 D Unfragmented DNA	3.88	1	>60	9	1	19	9	1	0.8
38 D Covaris- 300bp	1.59	1	16	1.9	3.1	7			

Bioanalyzer analysis showed that the DNA subjected to ultrasonication was successfully fragmented using the 300bp fragmentation protocol. The electropherogram result of the unfragmented DNA is shown in Figure 19.

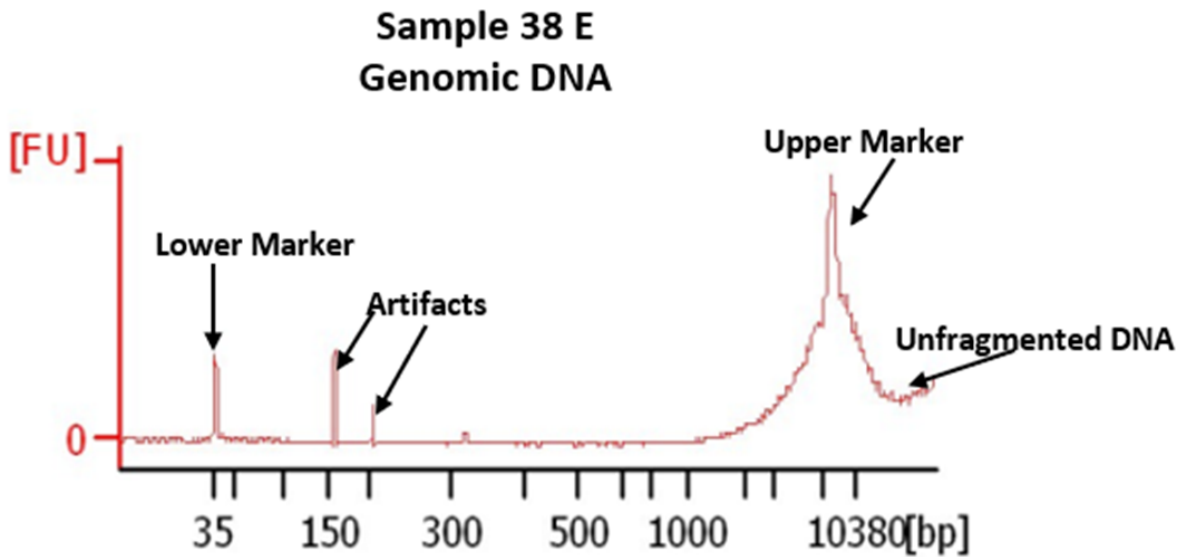


Figure 19: Electropherogram of unfragmented DNA extracted from human buffy coat. The peak beyond the upper marker (10380bp) shows unfragmented DNA. The peak at 35bp and 10,380bp indicates lower and upper marker, respectively.

The electropherogram results show a smooth line at the baseline between the lower (35bp) and upper (10,380) markers. Beyond the upper marker, there is an area of higher FU. The smooth lines between the 35bp and 10,380bp and the area of DNA larger than 10,380 represent unfragmented DNA. The image also shows two small peaks at 150bp and 250bp due to bubbles in the analysis. These peaks are artifacts.

Fragmentation of DNA was successful at 300bp but unsuccessful at 500bp. The electropherograms results are presented in Figure 20.

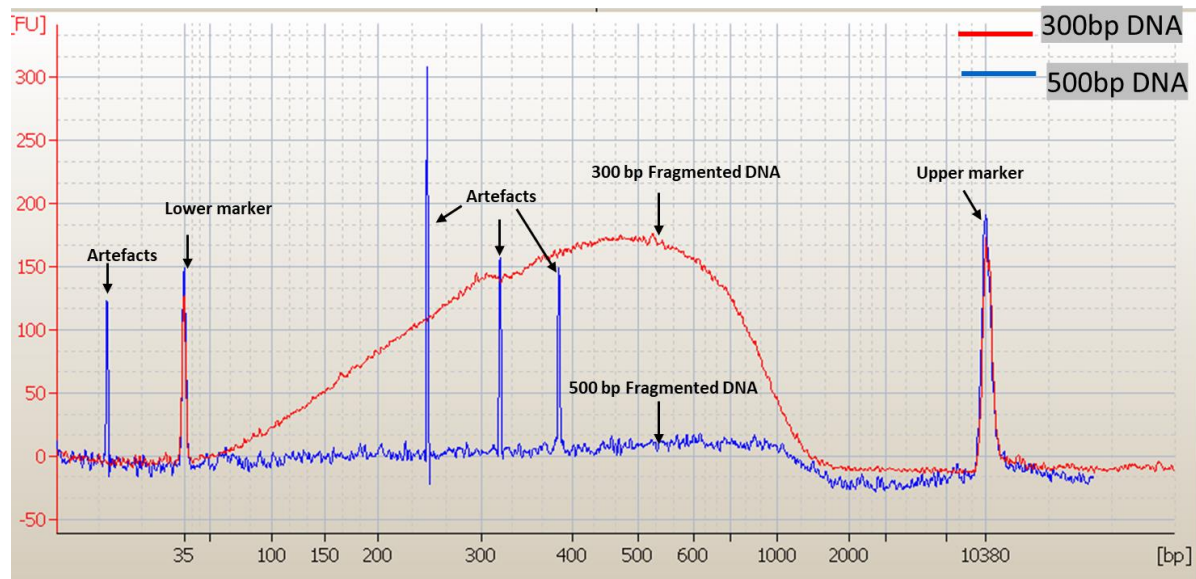


Figure 20: Electropherogram results of fragmented DNA extracted from human buffy coat. The red graph shows DNA fragmented using 300bp protocol, while the blue graph shows DNA fragmented using 500bp protocol. The 300bp protocol shows a normal distribution curve between the upper and lower markers. The 500bp protocol shows a slight peak in the graph however, the fragmentation was unsuccessful. The peak at 35bp and 10,380bp in both images indicates lower and upper marker, respectively.

The electropherogram results of 300bp DNA shown in Figure 20 (red) shows a normal distribution curve between 35bp and 10,380bp and verifies that DNA had produced fragments across this range, with a visible peak at 300bp and a Bioanalyser report of the average size of 472bp fragments. This verifies that the protocol to fragment DNA at 300bp was successful. DNA fragmentation at 500bp in Figure 20 (blue) was unsuccessful as there is no normal distribution curve or peak. The two small peaks at 150bp and 250bp are artefacts due to bubbles passing through the analysis chip.

Figure 21 shows the electropherogram result for the sample subjected to needle shearing and shows a slight curve from the baseline between the lower and upper markers, indicating partial fragmentation. The average size of fragmented DNA between the lower and upper marker shown by the graph is 236bp, while unfragmented DNA overlaying the upper marker is beyond 10,063bp.

Needle Shearing

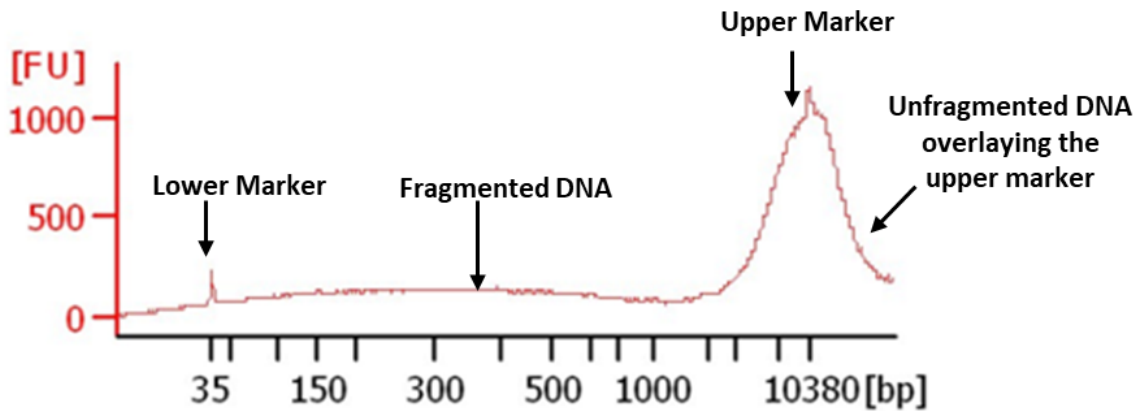


Figure 21: Electropherogram results of fragmented DNA extracted from human buffy coat. The peak at 35bp and 10,380bp indicates lower and upper marker, respectively. The slight curve between the two markers shows partial fragmentation. The unfragmented DNA is seen overlaying on the upper marker.

3.1.2 Analysis of Biotinylation of DNA via Agarose Gel

Results of agarose gel electrophoresis shown in Figure 22. This method was utilised based on the principle that the addition of biotin and streptavidin to DNA would slow the DNA migration during electrophoresis, producing a shift of DNA distribution when compared to the non-biotinylated DNA.

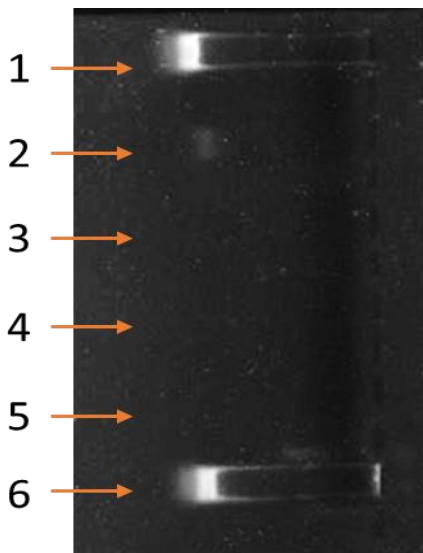


Figure 22: Gel-shift assay of biotinylated DNA-streptavidin dilutions via agarose gel electrophoresis. Image manipulated with contrast enhancement. Lane 1 and 6 represent a 1kp ladder, Lane 2 represents 300bp biotinylated DNA, Lane 3 represents biotinylated DNA -streptavidin at 1 in 5 dilutions, Lane 4 represents biotinylated DNA -streptavidin at 1 in 10 dilutions, Lane 5 represents biotinylated DNA -streptavidin at 1 in 20 dilutions. Visible bands could be seen in lane 1 and 6, while a light band could be seen in Lane 2.

The above result shows the band of 1 kbp ladder. However, the bands for biotinylated DNA with and without streptavidin could not be seen in the agarose gel as expected. It was not practical to repeat this experiment due to the limited quantity of biotinylated DNA sample.

3.2 Validation of Biotinylated DNA Fragments

3.2.1 Results of the minimum concentration of biotinylated polymers

Using the streptavidin-coated plate method, it was determined that Atri-PAA-Biotin could be detected at concentrations equal to or above 0.1 $\mu\text{g/mL}$. Results of the colourimetric detection technique using PNPP substrate are shown in Figure 23.

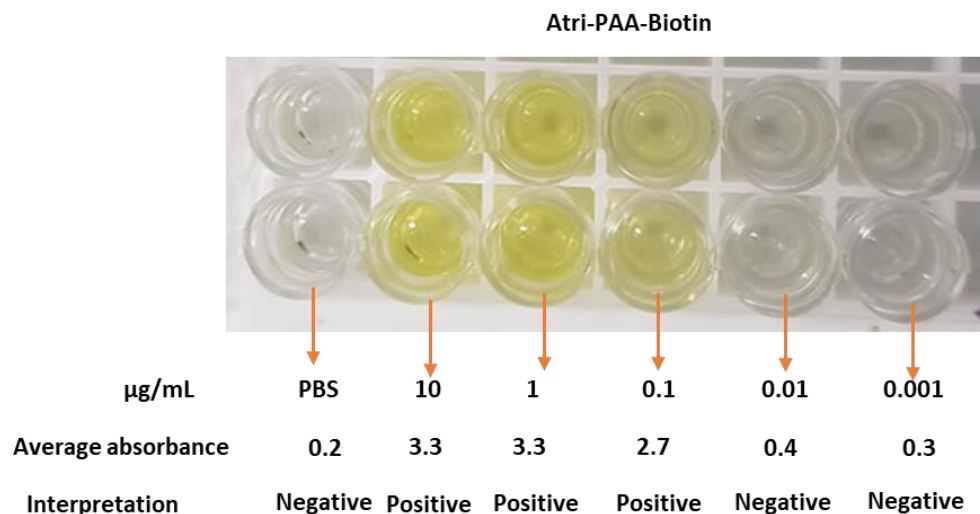


Figure 23: Colorimetric result of the reaction between enzyme streptavidin ALP and Atri-PAA-Biotin. The reactions were measured at 30 minutes post addition of substrate in the assay with varying concentrations of Atri-PAA-Biotin on streptavidin plate. PBS was blank and was used to compare the results with the other reaction wells. Atri-PAA-Biotin concentrations of 10 $\mu\text{g/mL}$, 1 $\mu\text{g/mL}$ and 0.1 $\mu\text{g/mL}$ showed a colour change from colourless to yellow (positive). While the Atri-PAA-Biotin concentrations of 0.01 $\mu\text{g/mL}$ and 0.001 $\mu\text{g/mL}$ showed no colour change (negative).

A second method with fluorescent signal confirmed that Atri-PAA-Biotin could be detected at concentrations equal to or above 0.1 $\mu\text{g/mL}$. Results are shown in Table 16.

Table 16: Fluorescent intensity excitation wavelength of 492 nm and an emission wavelength of 520 nm at 30 minutes at varying concentrations of Atri-PAA-Biotin on streptavidin plate. Readings are averages of all tests performed in duplicates. Readings above 16600 were considered positive.

Samples	Concentration μg/mL	Fluorescence Intensity	Interpretation
PBS	Blank	16651	Negative
Atri-PAA-Biotin	10 (No streptavidin AF)	15474	Negative
	10 (Streptavidin AF)	49386	Positive
	1	39296	Positive
	0.1	26745	Positive
	0.01	15666	Negative
	0.001	15710	Negative

Furthermore, a doubling dilution series of Atri-PAA-Biotin showed that concentrations as low as 0.01 μg/mL could be detected (Figure 24).

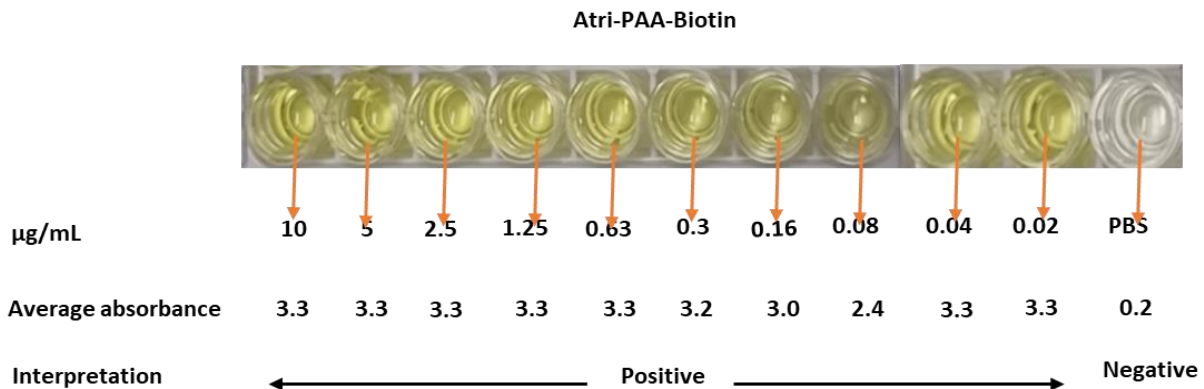


Figure 24: Colorimetric result of doubling dilutions of Atri-PAA-Biotin with enzyme streptavidin alkaline phosphatase on the streptavidin-coated plate. The reactions were measured at 30 minutes. PBS was blank and was used to compare the results with the other reaction wells. All concentrations of Atri-PAA-Biotin > 0.02 μg/mL were positive (yellow), while the PBS well remained colourless (negative).

However, with biotinylated DNA, concentrations of 1.25 $\mu\text{g/mL}$ and higher could be detected (**Error! Reference source not found.**).

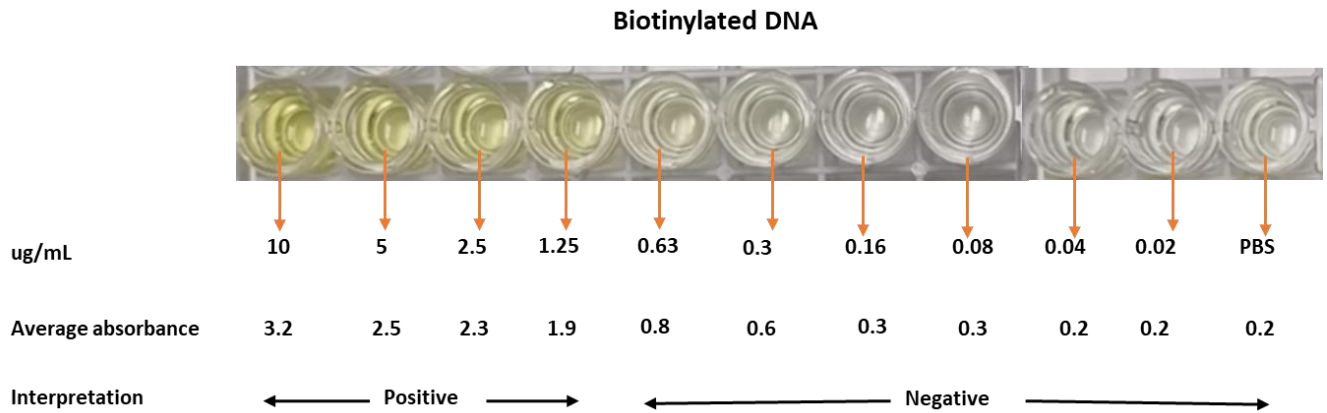


Figure 25: Colorimetric result of varying concentrations of biotinylated DNA with enzyme streptavidin alkaline phosphatase on the streptavidin-coated plate. The reactions were measured at 30 minutes. PBS was blank and was used to compare the results with the other reaction wells. Wells 1-4 (10 $\mu\text{g/mL}$, 5 $\mu\text{g/mL}$, 2.5 $\mu\text{g/mL}$ and 1.25 $\mu\text{g/mL}$) of biotinylated DNA were positive (changed yellow) while wells 5-10 including PBS well remained colourless (negative).

3.3 Validation of Biotin-Avidin Kodecytes

Results of the agglutination experiment conducted with streptavidin kodecytes loaded with Atri-PAA-Biotin are shown in Figure 26. Column 1 had no FSL-biotin and showed no agglutination (negative), column 2 had no streptavidin and showed no agglutination (negative), column 3 had no Atri-PAA-biotin and showed no agglutination (negative), and column 4 had FSL-biotin, streptavidin, Atri-PAA-Biotin and Anti-A and showed agglutination (positive). Agglutination proved that the polymer was present on the outside of the red cells and that a biotinylated polymer expressing the A antigen could be bridged to streptavidin kodecytes and agglutinated by Anti-A.

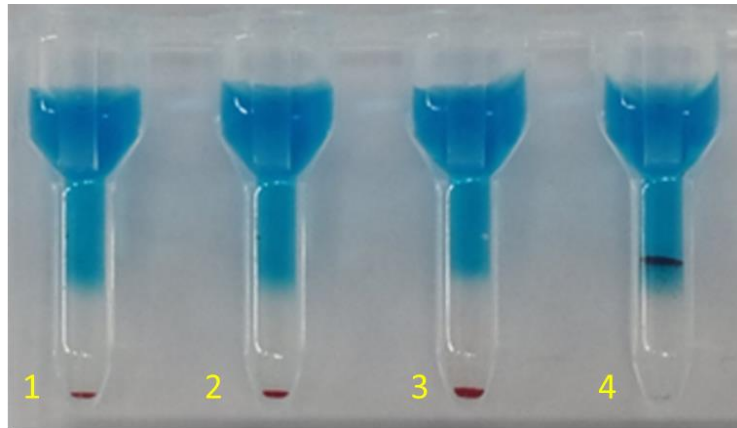


Figure 26: Column agglutination of streptavidin kodecytes. Column 1 had no FSL-Biotin and showed no agglutination (negative), column 2 had no streptavidin and showed no agglutination (negative), column 3 had no Atri-PAA-Biotin and showed no agglutination (negative), and column 4 had FSL-Biotin, Streptavidin, Atri-PAA-Biotin and Anti-A and showed agglutination (Positive).

3.4 Evaluating Mimic Reticulocytes

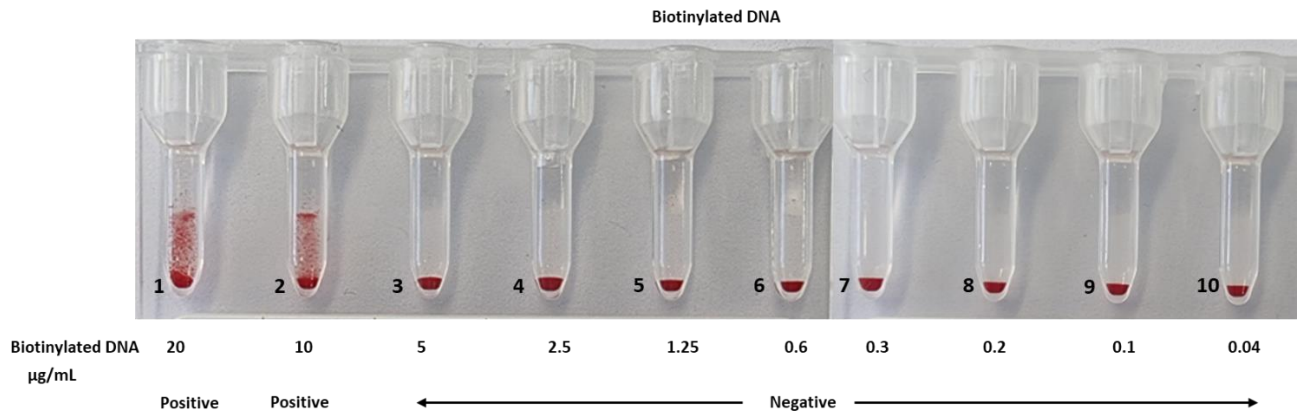


Figure 27: Column agglutination of mimic reticulocyte. Column 1 and 2 shows agglutination (positive) with streptavidin kodecytes and biotinylated DNA, while Columns 3-10, show no agglutination (negative).

Figure 27 shows aggregation of kodecyte prepared with biotinylated DNA at concentrations of 20 μg/mL and 10 μg/mL. Lower concentrations of biotinylated DNA did not result in kodecyte capable of aggregation. This means that at concentration 20 μg/mL and 10 μg/mL of biotinylated DNA, streptavidin on the kodecytes is still available for cross-linking and agglutination. If the concentration of biotinylated DNA were increased, then all the streptavidin sites on the kodecytes would have been bound by biotinylated DNA, therefore no cross-linking and agglutination would be seen. The negative results indicate that there is not enough biotinylated DNA to form cross-link between the streptavidin kodecytes and biotinylated DNA.

3.4.1 Analysis of Mimic Reticulocytes by Haematology Analyser and Supravital Staining

Results of mimic reticulocytes analysed using Sysmex analyser, and supravital stain is shown in Figure 28. Unmodified cells (image A and B) were used as a baseline to compare the modified cells (image C and D).

Unmodified cells were stained with brilliant cresyl blue (image A) and analysed using the Sysmex analyser (image B). The bluish-black inclusion in the marked cells (image A) represents RNA remnant as characteristically seen with this stain in reticulocytes⁽⁸⁾ however, the inclusion looks minimal. The manual count showed a reticulocyte count of 1.4%. Sysmex analysis yielded reticulocyte percentages of 3.86% for the unmodified red cells. The blue cloud in the scattergram (image B) indicates mature red blood cells, and the pink cloud represents the reticulocytes.

The unmodified cells were contaminated with 10% modified cells (mimic reticulocytes) and were analysed similarly to unmodified cells. The bluish-black inclusion in the marked cells (image C) represents RNA. Again, the inclusion looks minimal. The manual count showed a reticulocyte count of 1.5%. Furthermore, 100% modified cells were stained, and no inclusion could be seen on the cells (data not included). The Sysmex analysis yielded a reticulocyte percentage of 3.86%. The blue cloud in the scattergram (image D) indicates mature red blood cells, and the pink cloud represents the reticulocytes.

The stained smear, analyser reticulocyte percentage and scattergram results showed no difference between baseline (unmodified cells) and unmodified cells contaminated with 10% modified cells (mimic reticulocytes). It appears that the analyser detected only the natural reticulocytes in the unmodified cells only and did not detect the nucleic acid present on the mimic reticulocytes.

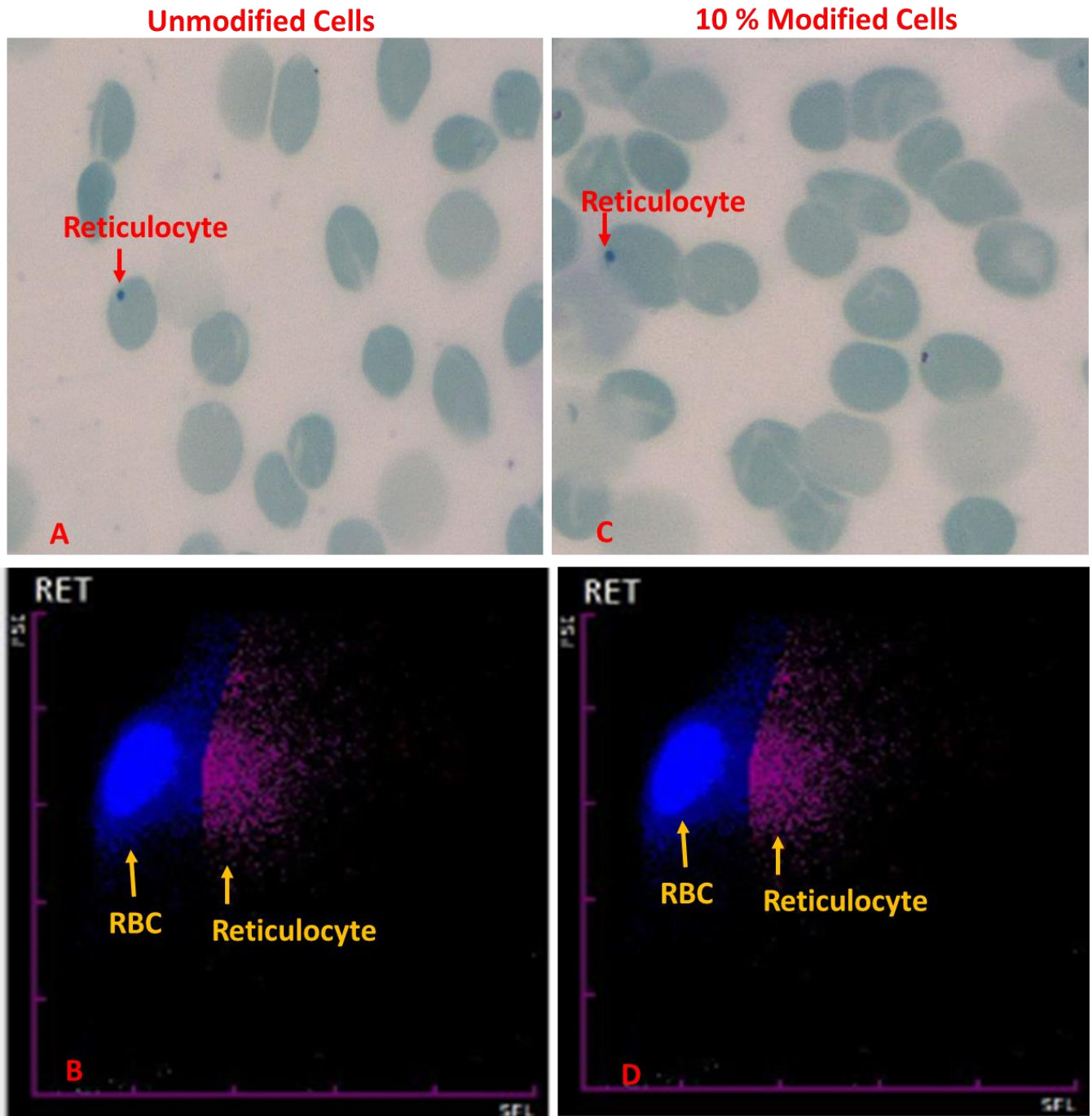


Figure 28: Sysmex analyser and BCB stain analysis. Image A (modified cells: mimic reticulocyte) and B (unmodified O cells) represent BCB stained cells with reticulocytes. Some red cells are darkly stained than the others. Image C represents the scattergram results, showing red blood cells in the blue cloud while reticulocytes in the pink cloud. The X-axis represents the side fluorescent scatter, and the Y-axis represents the forward scatter.

Various controls (Table 6) were run through the Sysmex analyser, but as they all yielded the same percentage of reticulocytes (in the region of 3.8%), scattergram figures are not presented here. Similarly, they all had the same appearance when BCB stained.

Some cells in image A and B are more lightly stained and slightly larger than others, which could mean the volume of the cell has increased, although the MCV results from the analyser did not support this.

4 Discussion

The reticulocyte count indicates the erythropoietic status of an individual, hence an accurate count of the number of reticulocytes in relation to the number of mature red cells is needed for clinical diagnosis, particularly in the area of anaemia⁽⁸⁾. Accurate, reproducible and reliable reticulocytes in the laboratory require the use of controls⁽⁴³⁾. Several commercial quality control kits are available for the manual or instrumental count of reticulocytes. These are normally prepared from human blood components⁽⁴³⁾. Because reticulocytes naturally undergo progressive maturation, the ability of control material of human blood cells to give a reproducible reticulocyte count during storage is reduced⁽⁴³⁾. This research aimed to investigate an alternative method of producing control using Kode technology to attach nucleic acid fragments to the surface of the red cells, which would aggregate as spots to prepare mimic reticulocytes that routine haematology methods could detect. To achieve this, four major steps were required. Firstly, DNA was prepared and fragmented. Secondly, fragmented DNA was biotinylated. This was followed by preparing biotin-avidin kodecytes and, lastly, capturing biotinylated DNA fragments on the biotin-avidin kodecytes to produce mimic reticulocytes that could be used by routine analysis. Each step was validated.

To prepare DNA, three different methods were evaluated, including a commercial kit and an “in-house” method with Proteinase K. In this research, efforts were made to optimise a suitable DNA extraction method for downstream fragmentation and biotinylation applications. When evaluating the DNA extraction options, considerations were sample type, purity of DNA, yield, time efficiency, storage requirements, and cost-effectiveness. The biggest limitation of this research was the availability of quality DNA.

Preparation of high-quality genomic DNA extraction from plant leaves with simple buffers proved challenging, as seen in Figure 18, Table 7, Table 9 and Table 10. This could be due to secondary metabolites in the plants (polysaccharides or polyphenol⁽⁸²⁾) or other contaminants that absorb light at 280 nm^(80, 83). The difference in results here compared to the literature could be due to the initial material used for DNA extraction. The authors of one published study⁽⁵⁵⁾ used different starting material of maize leaves, or *Arabidopsis* leaves. This research used spinach leaves, and the buffer chemicals used here may not have been potent enough to break the durable cell wall of spinach⁽⁸⁴⁾. The DNA kit used in this research uses silica-based membrane technology to bind selectively to DNA in the presence of chaotropic salts with the removal of impurities⁽⁵⁹⁾. Using the kit, it was possible to produce pure DNA (Table 12 and Table 13). However, although DNA concentration was consistent and higher than with buffer methods, the quantity was insufficient for downstream applications of fragmentation and biotinylation. Studies have shown that using commercial kits for DNA extraction yields pure DNA, but sometimes the quantity is low^(85, 86), as was seen in this study. Due to the consistent low yields from the commercial kit, it was decided to extract DNA

from a human buffy coat using the published method⁽⁵⁰⁾ utilizing detergent and proteinase K to extract DNA from the white cells of the buffy coat. Results showed high purity and concentration of total genomic DNA (Table 14) using this method. The results from this study are similar to other published works, thus providing great confidence in moving forward with the downstream application for this research⁽⁸⁷⁻⁸⁹⁾. It was anticipated that the DNA would need to be fragmented to enable its efficient coating of cells and allow for controlled labelling. It was decided that fragments > 300bp and < 1000bp should be optimal.

The genomic DNA extracted from the human buffy coat was broken up into smaller fragments using two methods: sonication and needle shearing. Sonication on the Covaris M220 Focused-ultrasonicator successfully produced DNA fragments of 300bp in reasonable quantities (Figure 19 image A and B). Needle shearing, a low-cost alternative to ultrasonication, was attempted but with limited success (Figure 21)

The second aspect of this research was to biotinylate the fragmented DNA. The biotinylation process allows the attachment of biotin to nucleic acids without changing their function⁽⁷³⁾. Since biotin has a strong interaction with streptavidin⁽⁴⁹⁾, it was used as the bridge to join biotinylated DNA to FSL-Biotin kodeocytes. Two methods were used to assess the success of DNA biotinylation; traditional gel electrophoresis and binding to the streptavidin-coated plate. Although gel electrophoresis was a reasonable way to assess this, based on the different size and mobility of DNA versus biotinylated DNA⁽⁷²⁾, it was not successful in this instance (Figure 22). Reasons for the method failure could include a low concentration of DNA or alternatively long fragments producing steric hindrance⁽⁷²⁾.

The streptavidin-coated plate method proved successful to show that DNA was biotinylated (**Error! Reference source not found.**). Before being able to prove the success of DNA biotinylation, a surrogate of Atri-PAA-Biotin was introduced. Using a surrogate allowed this research to optimize protocols before consuming limited biotinylated DNA. Atri-PAA-Biotin is a biotinylated polymer including blood group A antigen⁽⁷⁵⁾. It is a blood group A trisaccharide antigen coupled with polyacrylamide spacer and biotin (Atri-PAA-Biotin)⁽⁷⁵⁾ shown in Figure 11. Polyacrylamide provides hydrophilicity, flexibility that increases the polymeric chain's affinity to binding proteins, is stable in a chemical environment, and stable in enzymatic reactions⁽⁷⁵⁾. In addition, the biotin in the polymer has a high affinity to streptavidin⁽⁷⁵⁾. It has approximately ten biotin molecules, thus determining the streptavidin concentration to be added in excess⁽⁷⁵⁾. The Atri-PAA-Biotin has a similar molecular weight as the 300bp biotinylated DNA used for this research. In addition, the Atri-PAA-Biotin polymer expresses blood group A antigen which made it useful in detection as it binds to anti-A antibody.

Atri-PAA-Biotin was used both to optimize methodology for assessment of polymer biotinylation and to determine the concentration and volume of biotinylation of DNA needed later to make mimic reticulocytes.

Assessing Atri-PAA-Biotin's binding to streptavidin was detected by ELISA methods based on both colourimetric and fluorescence detection. Both detection methods generated a signal with concentrations of Atri-PAA-Biotin as low as 0.1 µg/mL, as shown in Figure 23 and Table 16. In contrast, with 300bp biotinylated DNA, the lowest detectable concentration was 1.25 µg/mL (**Error! Reference source not found.**). The difference could be due to how biotin on the polymers presents itself. Atri-PAA-Biotin is a flexible molecule allowing increased affinity between the binding protein and glycan⁽⁷⁵⁾, therefore allowing biotin to present itself to streptavidin AF in any way.

On the other hand, DNA is less flexible⁽⁹⁰⁾, leading to biotin being hidden within the structure and not being as available to streptavidin for binding. Both detection methods proved that streptavidin immobilized on a polystyrene plate could bind to a biotinylated polymer and be analysed in this modified ELISA method, but the method was more sensitive for Atri-PAA-Biotin than it was for biotinylated DNA. The use of the model of the biotinylated polymer established methods that proved FSL-biotin kodeocytes can capture biotinylated molecules via streptavidin bridging. Subsequently, the same method was used to successfully prove that DNA was biotinylated (**Error! Reference source not found.**).

The third aspect of the research was to validate that biotin kodeocytes had bound streptavidin. To prove the concept, Atri-PAA-Biotin was again used as a surrogate. Using an agglutination method, it was proved that Atri-PAA-biotin binds to biotin kodeocytes via streptavidin bridge, as shown in Figure 26. Agglutination proved that a biotinylated polymer expressing the A antigen (blood group Atri) could be bridged to streptavidin kodeocytes and agglutinated by monoclonal IgM Anti-A.

The use of Atri-PAA-Biotin proved that biotinylated polymers could bind to streptavidin. Furthermore, it also proved that FSL-Biotin could capture the biotinylated polymer via streptavidin as a bridge. Finally, due to the limited amounts (300bp biotinylated DNA) of the final product, using the biotinylated polymer provided some insight into the volumes and concentrations needed for the reactions.

Therefore, using all the above information, the last aspect of this research evaluating mimic reticulocytes was performed. The hypothesis for the current study that streptavidin could form a bridge between biotin kodeocytes and 300bp biotinylated DNA was proved via the aggregation method. This hypothesis was first assessed using surrogate polymer Atri-PAA-Biotin (Figure 26). The FSL-biotin kodeocytes were saturated with streptavidin by adding excess. The addition of streptavidin in excess allowed streptavidin to be available to biotin on the Atri-PAA-Biotin only, proving the biotinylated polymer (Atri-PAA-Biotin) can

be attached to the biotin kodeocytes via streptavidin. However, due to insufficient biotinylated DNA sample, the experiment could not be performed similarly to Atri-PAA-Biotin.

The results in Figure 27 showed higher concentrations of biotinylated DNA aggregated on the red cells while the lower concentrations did not. Again, no aggregation in a lower concentration of biotinylated DNA could be attributed to how biotin in DNA is presented for the streptavidin binding. Alternatively, there may have been insufficient biotinylated DNA to cross-link between the streptavidin kodeocytes and biotinylated DNA. If the concentration of biotinylated DNA were increased, then all the streptavidin sites on the kodeocytes would have been bound by biotinylated DNA, therefore no cross-linking and agglutination would be seen. Studies have biotinylated DNA at one terminus of the DNA fragment to prevent cross-linking between DNA bridges resulting in poor reactions between the molecules and the detection method^(91, 92). For this research, the biotinylation technique was nick translation and could have affected how biotin is presented to the streptavidin. A study used silica beads to detect the presence of biotinylated DNA^(91, 92).

The mimic reticulocytes were analysed using the Sysmex analyser and then visualised using supravital stain (BCB). The analyser did not give any abnormal reticulocyte scattergram or reticulocyte flags. This means that the analyser was able to process the modified cells as normal cells. The Sysmex analyser count indicated the presence of reticulocytes, which correlated with the reticulocyte scattergram cloud shown in Figure 28. In addition, the presence of reticulocytes was also evident in the BCB stained smear. However, the results between the unmodified natural cells and the mimic reticulocytes yielded the same reticulocyte percentages, and so it appears that the analyser cannot “see” the mimic reticulocytes. This could be due to several reasons. Firstly, the mimic reticulocytes were prepared by attaching DNA to the surface of the cells, while natural reticulocytes have RNA inside the cell⁽⁸⁾. When the cells are analysed in the Sysmex analyser, the diluent (CellPack DFL) makes the cell membrane permeable⁽⁶⁾. Once the cell membrane becomes permeable, the fluorocell RET dye enters the cells and stains the nuclear and granular contents of the cells⁽⁶⁾. In a natural reticulocyte, the RNA would be stained, and RBC would show limited staining due to the small amount of organelle remaining. For this research, since the DNA was attached to the cells' surface, it is difficult to know whether the fluorocell RET bound the surface DNA. Furthermore, the diluent used in the Sysmex model XN-20 contains a surfactant to render the cells permeable to allow the dye to enter the cell⁽⁶⁾. Kodeocytes rely on the attachment of FSL to red cells by insertion of the lipid-rich glycocalyx⁽⁴⁹⁾. Surfactants with a concentration of >1% in the diluents are likely to strip FSL out of the red cell⁽⁴⁹⁾. Further research is required to evaluate the effect of surfactant on labelling. However, the mimic kodeocytes assay is dependant on the FSL-Biotin-biotinylated DNA fragments clustering on the surface of the kodeocytes (facilitated by the dye). It is probable this did not happen, and further research is required.

Secondly, the Sysmex analyser measures the fluorescent labelled cell in the flow cell using forward light scatter (FSC) and side fluorescent light (SFL)⁽⁶⁾. The FSC represents the cell volume, while the SFL represents RNA and cell organelle in the reticulocyte⁽⁶⁾. The analyser differentiates the reticulocytes from the mature RBC as the reticulocytes retain the highly fluorescent RNA in the cytoplasm⁽⁶⁾. Since the DNA is attached to the cell surface in this research rather than being present in the cell cytoplasm, the analyser may not be optimal for detecting surface-attached DNA (especially if not aggregated). A study has suggested that protein/antibody-conjugated DNA labelled with fluorescent probes⁽⁷²⁾ can be detected with flow cytometry. However, the techniques of the flow cytometry reported in that study⁽⁷²⁾ are not the same as the light scatter principles utilised by the flow cell in the Sysmex analyser⁽⁹³⁾

The Sysmex was not able to enumerate the mimic reticulocytes. Nor was supravital staining able to demonstrate the presence of the nucleic acid on the surface of the red cells. In natural reticulocytes, the RNA remnants are visualised when supravital dyes such as brilliant cresyl blue diffuse into the cell and bind to RNA⁽⁹⁴⁾. Amongst the natural cells, reticulocytes were seen (Figure 28). This was not unexpected, as all adults have some reticulocytes present⁽⁸⁾, and the Sysmex analysis reported 3.6% of red cells were reticulocytes in the natural cells. However, it was hoped higher numbers of cells containing stained reticular structures would be seen in the mimic reticulocytes preparation. This was not the case here (Figure 28).

Reasons for failure to detect DNA on mimic reticulocytes by supravital staining could include attachment of DNA to the cell's surface. When cells (both unmodified and modified as mimic reticulocytes) were stained with BCB, some cells appeared slightly larger and lighter stained than normal red cells. The increase in size could be due to the packed red cells stored in preservatives. Due to the size increase, the haemoglobin appears less thus, cells stained lighter than usual. Studies have shown red cell volume increases when stored in preservatives^(95, 96).

The method design to prepare mimic reticulocytes is not necessarily flawed, but further method optimisation would need to be undertaken to prove that it can work, particularly the induction of aggregation of the DNA on the surface. Due to limited biotinylated DNA, there was no opportunity to test different concentrations of all prepared “reagents” of DNA fragments, biotinylated DNA and streptavidin. All these require optimisation to establish the optimal biotin-streptavidin ratio to prepare the mimic reticulocytes for visualisation in the haematology analyser and/or the supravital stain. Unfortunately, further optimisation steps were not possible during this research due to time constraints.

In future research, a different biotinylation method approach could be tried, using 5' biotinylated DNA fragments instead of biotinylation via nick translation. The 5' biotinylation might allow linear DNA to extend out of the cell⁽⁷²⁾ and be detected via staining (fluorescence light scatter or supravital).

Furthermore, to assess the success of method steps prior to analysis in the haematology analyser, fluorescent dyes could be used⁽⁹⁷⁾. The dye of BCB does have fluorescent properties and provides use as a conventional supravital stain⁽⁹⁷⁾. Consideration was given to preparing mimic reticulocytes stained with BCB and viewing them under a fluorescence microscope, but this was not possible as the biotinylated DNA sample was exhausted.

Lastly, assuming mimic reticulocytes could be made successfully, the stability and reproducibility of the mimic reticulocytes would need to be tested to assess the suitability of mimic reticulocytes as a control for haematology laboratories.

In conclusion, this research had partial success. The DNA was successfully extracted, fragmented and biotinylated. A novel method for demonstrating that biotinylated polymers could bind red cells coded with biotin via streptavidin bridge was successful. However, although the final aim of producing red cells loaded with DNA was able to be successfully demonstrated, they did not behave as mimic reticulocytes by either a haematology analyser or supravital staining.

Reference

1. Moras M, Lefevre SD, Ostuni MA. From erythroblasts to mature red blood cells: organelle clearance in mammals. *Frontiers in physiology* [internet]. 2017 [cited 2021] 19;8(1076). Available from: <https://doi.org/10.3389/fphys.2017.01076>
2. Rai D, Wilson AM, Moosavi L. *Histology, reticulocytes* [Internet]. Treasure Island: StatPearls Publishing; 2021 Feb [updated 2021 Feb 19; cited 2021 Feb]. Available from: <https://www.ncbi.nlm.nih.gov/books/NBK542172/>
3. Du R, Bei H, Jia L, Huang C, Chen Q, Wang J, et al. A low-cost, accurate method for detecting reticulocytes at different maturation stages based on changes in the mitochondrial membrane potential. *Journal of pharmacological and toxicological methods* [internet]. [update 2020 Jan-Feb cited 2021] 101:106664. Available from: <https://doi.org/10.1016/j.vascn.2019.106664>
4. Sung HH, Seok DI, Jung YH, Kim DJ, Lee SJ. Experience of reticulocytes measurement at 720 nm using spectrophotometer. *Korean journal of clinical laboratory science* [internet]. 2017 Dec [cited 2021] 31;49(4):382-9. Available from: <https://doi.org/10.15324/kjcls.2017.49.4.382>
5. Piva E, Brugnara C, Spolaore F, Plebani M. Clinical utility of reticulocyte parameters. *Clinics in laboratory medicine* [internet]. 2015 [cited 2021] 35(1):133-63. Available from: <http://dx.doi.org/10.1016/j.cll.2014.10.004>
6. Sysmex educational enhancement and development. The importance of reticulocyte detection [internet]. Germany: Sysmex Europe GmbH; 2016 [updated 2016 Jan; cited 2021 Feb]. Available from: <https://www.sysmex-wca.com/academy/library/xtra/seed-the-importance-of-reticulocyte-detection-25441.html>
7. Moradabadi A, Khaleghi M, Shahdoost M, Farsinejad A. Optimized method for reticulocyte counting: simple, accurate, and comparable to flow cytometry. *Iranian journal of pediatric haematology and oncology* [internet]. 2019 [cited 2021] 9(1):17-24. Available from: <http://dx.doi.org/10.18502/ijpho.v9i1.292>
8. Riley RS, Ben-Ezra JM, Goel R, Tidwell A. Reticulocytes and reticulocyte enumeration. *Journal of clinical laboratory Analysis* [internet]. 2001 Sep [cited 2021] 20;15(5):267-94. Available from: <https://doi.org/10.1002/jcla.10399>.
9. Ryan WL, Ebrahim A. (1995). Reference control for use with manual and flow cytometric reticulocyte counting devices. US Patent Number 5432089 Streck Laboratories Inc.
10. Riley RS, Ben-Ezra, Jonathan M, Tidwell A. Reticulocyte enumeration: past & present. *Laboratory medicine*[internet].2001 Oct [cited 2021] 32(10):599-608. Available from: https://www.habx.in/habx_admin/assets/uploads/P120-RET_2001-Riley_Retic_LabMedicine-10-vol-32-1.pdf

11. Lin CK, Chiu CF, Kuo BI, Lin FM, Jiang ML, Chow MP. Do the reticulocyte maturation fractions and bone marrow reticulocyte count further help the classification of anaemias? *Zhonghua Yi Xue Za Zhi* [internet]. 1994 May [cited 2021] 53(5):270-5. Available from: <https://pubmed.ncbi.nlm.nih.gov/8039039/>
12. El-Lahony DM, Saleh NY, Habib MS, Shehata MA, El-Hawy MA. The role of recombinant human erythropoietin in neonatal anemia. *Hematology/oncology and stem cell therapy* [internet]. 2020 Sep [cited 2021] 3(13):147-51. Available from: <https://doi.org/10.1016/j.hemonc.2019.08.004> .
13. Hiradfar A, Banihosseinian M. The efficacy of recombinant human erythropoietin in treatment chemotherapy induced anemia in children diagnosed with a solid cancer. *Iranian journal of pediatric hematology & oncology* [internet]. 2014 Dec [cited 2021] 10;4(4):151-59. Available from: <https://www.ncbi.nlm.nih.gov/pmc/articles/PMC4293514/pdf/ijpho-4-151.pdf>
14. Clinical and laboratory standards Institute. Methods for reticulocyte counting (automated blood cell counters, flow cytometry, and supravital dyes). *NCCLS* [internet]. 2004 Feb [cited 2021] 24(8). Available from: <https://demo.nextlab.ir/getattachment/37cc5b50-33c7-401c-9ce9-92435c598163/CLSI-H44-A2.aspx>
15. Pierre RV. Reticulocytes: their usefulness and measurement in peripheral blood. *Clinics in laboratory medicine* [internet]. 2002 Mar [cited 2021] 01; 22(1):63-79. Available from: [https://doi.org/10.1016/s0272-2712\(03\)00067-2](https://doi.org/10.1016/s0272-2712(03)00067-2)
16. Hüntelmann AC. Staining is the best policy“. Visualization in the work of Paul Ehrlich. *Berichte zur Wissenschaftsgeschichte* [internet]. 2013 Dec [cited 2021] 02;36(4):354-80. Available from: <https://doi.org/10.1002/bewi.201301648>
17. Erb W. Zur Entwicklungsgeschichte der rothen Blutkörperchen. *Archiv für pathologische Anatomie und Physiologie und für klinische Medicin*. 1865;34(1-2):138-93. Available from: <https://link.springer.com/article/10.1007/BF02254539>
18. Smith T, Kilborne FL. Investigations into the nature, causation, and prevention of Texas or southern cattle fever [internet]. United states of America; US Government Printing Office; 1893. Available from: <http://resource.nlm.nih.gov/62350480R>
19. Viana KA, Filho OA, Dusse LA, Avelar RS, Avelar DV, Carvalho B, et al. Reticulocyte count: comparison among methods. *Laboratory medicine* [internet]. 2014 Sep/Oct [cited 2021] 50(5):339-45. Available from: <https://doi.org/10.5935/1676-2444.20140037>
20. Piva E, Brugnara C, Chiandetti L, Plebani M. Automated reticulocyte counting: state of the art and clinical applications in the evaluation of erythropoiesis. *Clinical chemistry and laboratory medicine* [internet]. 2010 Jul [cited 2021] 29; 48(10):1369-80. Available from: <https://doi.org/10.1515/CCLM.2010.292>
21. Celkan TT. What does a hemogram say to us? *Turk Pediatri Ars* [internet]. 2020 Jun [cited 2021] 19;55(2):103-16. Available from: <https://dx.doi.org/10.14744/2FTurkPediatriArs.2019.76301> .
22. Kosenow W, Mai H. Fluorescence microscopy of blood cells. *Zeitschrift für Kinderheilkunde* [internet]. 1952 [cited 2021] 70(6):552-60. Available from: <https://pubmed.ncbi.nlm.nih.gov/12995805/>

23. Nazi KM. The Miller Disk: an improvement in the performance of manual reticulocyte counts. *Laboratory medicine* [internet]. 1986 [cited 2021]17(12):742-4. Available from: <https://doi.org/10.1093/labmed/17.12.742>
24. Buttarello M. Laboratory diagnosis of anaemia: are the old and new red cell parameters useful in classification and treatment, how? *International journal of laboratory haematology* [internet]. 2016 May [cited 2021] 16;38 (S1):123-32. Available from: <https://doi.org/10.1111/ijlh.12500>
25. Arneth BM, Menschikowki M. Technology and new fluorescence flow cytometry parameters in hematological analyzers. *Journal of clinical laboratory analysis* [internet]. 2015 [cited 2021] 29(3):175-83. Available from: <https://doi.org/10.1002/jcla.21747>
26. Green R, Wachsmann-Hogiu S. Development, history, and future of automated cell counters. *Clinical laboratory Medicine* [internet]. 2015 [cited 2021] 35(1):1-10. Available from: <http://dx.doi.org/10.1016/j.cll.2014.11.003>
27. Beckman Coulter Inc. Coulter HmX haematology analyzer [pamphlet]. United States Beckman Coulter; 2011
28. Beckman Coulter Inc. Technology and case studies: DxH 500 series haematology analyser [pamphlet]. United States Beckman Coulter; 2018
29. Beckman Coulter life series. Coulter principle, counting and sizing particles [internet]. Australia: Beckman Coulter 2021. Available from: <https://www.beckman.com/resources/fundamentals/history-of-flow-cytometry/the-coulter-principle>.
30. Coulter. Coulter® VCS reticulocyte method [internet]. United States of America: Coulter international corporation 1996 [Available from: <http://www.cyto.purdue.edu/cdroms/cyto2/6/coulter/ss000126.htm>].
31. Maciel TS, Comar SR, Beltrame MP. Performance evaluation of the Sysmex® XE-2100D automated haematology analyzer. *Journal brasileiro de patologia e medicina laboratorial* [internet]. 2014 Feb [cited 2021]50(1):26-35. Available from: <https://doi.org/10.1590/S1676-2444201400010000434>.
32. Sysmex Corporation. Principle for measuring reticulocytes with XE-5000 and XE-2100, making use of bioimaging technology. Sysmex corporation [internet]. 2007 [cited 2021] Available from: https://www.sysmex.at/fileadmin/media/f103/Scientific_Bulletins/ScientificBulletin_Part3.pdf.
33. Huh J, Moon H, Chung W. Erroneously elevated immature reticulocyte counts in leukemic patients determined using a Sysmex XE-2100 hematology analyzer. *Annals of haematology* [internet]. 2007 [cited 2021]86(10):759-62. Available from: <https://doi.org/10.1007/s00277-007-0314-641>.
34. Grotto HW. Platelet and reticulocyte new parameters: why and how to use them? *Revista brasileira de hematologia e hemoterapia* [internet]. 2016 Oct/Dec [cited 2021]38(4):283-4. Available from: <https://doi.org/10.1016/j.bjhh.2016.08.001>

35. Nobes PR, Carter AB. Reticulocyte counting using flow cytometry. *Journal Of Clinical Pathology* [internet]. 1990 [cited 2021]43(8):675-8. Available from: <http://dx.doi.org/10.1136/jcp.43.8.675>
36. Davis B. Immature reticulocyte fraction (IRF): by any name, a useful clinical parameter of erythropoietic activity. *Laboratory haematology* [internet]. 1996[cited 2021]2:2-8. Available from <https://pubmed.ncbi.nlm.nih.gov/9208980/>
37. Gonçalo AP, Barbosa IL, Campilho F, Campos A, Mendes C. Predictive value of immature reticulocyte and platelet fractions in hematopoietic recovery of allograft patients. *Transplantation proceedings* [internet]. 2011 Jan/Feb[cited 2021]43(1):241-3. Available from: <https://doi.org/10.1016/j.transproceed.2010.12.030>.
38. Petegem M, Cartuyvels R, Schouwer P, Duppen V, Goossens W, Hove L. Comparative evaluation of three flow cytometers for reticulocyte enumeration. *Clinical & Laboratory Haematology* [internet]. 1993 Jun [cited 2021]15(2):103-11. Available from: <https://doi.org/10.1111/j.1365-2257.1993.tb00133.x>
39. Johnson AM. (2002). Reticulocyte containing complete blood control. US patent number 6444471B1. Research & diagnostic systems, Inc.
40. Salle BD. Survey material choices in haematology EQA: a confounding factor in automated counting performance assessment. *Biochem Med* [internet]. 2017 [cited 2021] 27(1):63-72. Available from: <https://doi.org/10.11613/BM.2017.008>
41. Henry SM, Bovin NV. Kode Technology—a universal cell surface glycan modification technology. *Journal of the royal society of New Zealand* [internet]. 2019 [cited 2021] 49(2):100-13. Available from: <https://doi.org/10.1080/03036758.2018.1546195>
42. Henry SM, Perry H, Bovin NV. Applications for kodecytes in immunohaematology. *ISBT Science Series* [internet]. 2018 [cited 2021]13(3):229-37. Available from: <https://doi.org/10.1111/voxs.12403>
43. Korchagina E, Tuzikov A, Formanovsky A, Popova I, Henry SM, Bovin NV. Toward creating cell membrane glyco-landscapes with glycan lipid constructs. *Carbohydrate research* [internet]. 2012 Jul 15 [cited 2021] 356:238-46. Available from: <https://doi.org/10.1016/j.carres.2012.03.044>
44. Frame T, Carroll T, Korchagina E, Bovin NV, Henry SM. Synthetic glycolipid modification of red blood cell membranes. *Transfusion* [internet]. 2007 May [cited 2021] 47(5):876-82. Available from: <https://doi.org/10.1111/j.1537-2995.2007.01204.x>
45. Henry SM. Modification of red blood cells for laboratory quality control use. *Current Opinion in Haematology* [internet]. 2009 Nov [cited 2021]16(6):467-72. Available from: <https://doi.org/10.1097/MOH.0b013e328331257e>
46. Henry SM, Williams E, Barr K, Korchagina E, Tuzikov A, Ilyushina N, et al. Rapid one-step biotinylation of biological and non-biological surfaces. *Scientific reports* [internet]. 2018 Feb 18 [cited 2021] 8(1):2845. Available from: <https://doi.org/10.1038/s41598-018-21186-3>

47. Qamar W, Khan MR, Arafah A. Optimization of conditions to extract high quality DNA for PCR analysis from whole blood using SDS-proteinase K method. Saudi journal of biological sciences [internet]. 2017 Nov [cited 2021] 24(7):1465-9. Available from: <https://doi.org/10.1016/j.sjbs.2016.09.016>
48. Tan SC, Yiap BC. DNA, RNA, and Protein Extraction: the past and the present. Journal of biomedicine and biotechnology [internet]. 2009 [cited 2021] 574398. Available from: <https://doi.org/10.1155/2009/574398>
49. Pitcher D, Saunders N, Owen R. Rapid extraction of bacterial genomic DNA with guanidium thiocyanate. Letters in applied microbiology [internet]. 1989 April [cited 2021] 8(4):151-6. Available from: <https://doi.org/10.1111/j.1472-765X.1989.tb00262.x>
50. Alonso A. DNA Extraction and Quantification. Encyclopedia of Forensic Sciences [internet]. 2013 [cited 2021]. p. 214-8. Available from: 10.1016/B978-0-12-382165-2.00039-8
51. Chabi SK, Kefela T, Adoukonou SH, Ahoton L, Saidou A, Baba ML, et al. A simple and efficient genomic DNA extraction protocol for large scale genetic analyses of plant biological systems. Plant Gene [internet]. 2015 Mar [cited 2021] 1:43-5. Available from: <https://doi.org/10.1016/j.plgene.2015.03.001>
52. Lu Y. Extract genomic DNA from Arabidopsis leaves (Can be used for other tissues as well). Bio-protocol [internet]. 2011 [cited 2021];1(13):e90. Available from <https://bio-protocol.org/bio101/e90>
53. Deshmukh VP, Thakare PV, Chaudhari US, Gawande PA. A simple method for isolation of genomic DNA from fresh and dry leaves of Terminalia arjuna. Electronic journal of biotechnology [internet]. 2007 [cited 2021]10(3):468-72. Available from: <https://doi.org/10.2225/vol10-issue3-fulltext-5>
54. Sahu SK, Thangaraj M, Kathiresan K. DNA extraction protocol for plants with high levels of secondary metabolites and polysaccharides without using liquid nitrogen and phenol. Molecular Biology [internet]. 2012 [cited 2021] 205049. Available from: <https://doi.org/10.5402/2012/205049>
55. New England Biolabs. DNA Precipitation: Ethanol vs. Isopropanol [internet]. New England: Bitesize Bio marketing; 2015. Available from: <https://bitesizebio.com/2839/dna-precipitation-ethanol-vs-isopropanol/>.
56. ThermoFisher scientific invitrogen in life technologies. PureLink® Plant Total DNA Purification Kit [internet]. United States of America: 27 September 2012; [cited 2021]. Available from: <https://www.thermofisher.com/document-connect/document-connect.html>
57. Palmirotta R, Ludovici G, De-Marchis ML, Savonarola A, Leone B, Spila A, et al. preanalytical procedures for DNA Studies. Biopreservation and biobanking [internet]. 2011 Apr 07 [cited 2021] 9(1):35-45. Available from: <https://doi.org/10.1089/bio.2010.0027>
58. Sambrook J, Green MR. Molecular cloning: a laboratory manual [internet]. New York: Cold spring harbour laboratory press; 2012; [cited 2021]. Available from: <https://www.cshlpress.com/pdf/sample/2013/MC4/MC4FM.pdf>

59. Ponti G, Maccaferri M, Manfredini M, Kaleci S, Mandrioli M, Pellacani G, et al. The value of fluorimetry (Qubit) and spectrophotometry (NanoDrop) in the quantification of cell-free DNA (cfDNA) in malignant melanoma and prostate cancer patients. *Journal of clinical chemistry* [internet]. 2018 April [cited 2021];479:14-9. Available from: <https://doi.org/10.1016/j.cca.2018.01.00762>.
60. Nakayama Y, Yamaguchi H, Einaga N, Esumi M. Pitfalls of DNA quantification using DNA-binding fluorescent dyes and suggested solutions. *PLoS One* [internet]. 2016 Mar 03 [cited 2021] 11(3):e0150528. Available from: <https://doi.org/10.1371/journal.pone.0150528>
61. Invitrogen by Life Technologies. Qubit 2.0 Fluorometer [internet]. United States of America: Invitrogen; 2010 [updated 04 october 2010; cited 2021]. Available from: https://www.mbl.edu/jbpc/files/2014/05/Qubit2_Fluorometer_UserManual.pdf.
62. Invitrogen Life Technologies. BioNick™ Labeling System [internet]. 2003 [cited 2021]. Available from: https://assets.thermofisher.com/TFS-Assets/LSG/manuals/bionick_man.pdf.
63. Green DJ, Rudd EA, Laugharn JA. Adaptive Focused Acoustics (AFA) improves the performance of microtiter plate ELISAs. *Journal of biomolecular screening* [internet]. 2014 Feb 19 [cited 2021]19(7):1124-30. Available from: <https://doi.org/10.1177/1087057114523650>
64. Shen KC, Kakumanu S, Beckett CD, Laugharn JA. Use of Adaptive Focused Acoustics™ ultrasound in controlling liposome formation. *Ultrasonics Sonochemistry* [internet]. 2015 Nov [cited 2021] 27:638-45. Available from: <https://doi.org/10.1016/j.ultsonch.2015.04.027>
65. Tyson J. Modified LSK109 ligation prep with needle shear and bead clean up [internet]. Canada: Snutch lab; 30 January 2020 [cited 2021]. Available from: [dx.doi.org/10.17504/protocols.io.7emhjc6](https://doi.org/10.17504/protocols.io.7emhjc6)
66. Centre for Molecular Medicine and Therapeutics. Principles of Sample Analysis on a Chip.: Adapted from the Agilent 2100 expert software online help [internet]. British Columbia: Center of molecular medicine and therapeutics; 11 2003 [cited 2021]. Available from: <https://cmmt.ubc.ca/facilities-services/bioanalyzer/principles-of-sample-analysis-on-a-chip/>
67. Nachamkin I, Panaro NJ, Li M, Ung H, Yuen PK, Kricka LJ, et al. Agilent 2100 bioanalyzer for restriction fragment length polymorphism analysis of the *Campylobacter jejuni* flagellin gene. *Journal of clinical microbiology* [internet]. 2001 Feb [cited 2021] 39(2):754-757. Available from: <https://doi.org/10.1128/JCM.39.2.754-757.2001>
68. Klevan L, Gebeyehu G, Rao PY. (1989). Nucleotide analogs for nucleic acid labeling and detection. US patent number 4828979. Life technologies, Inc.
69. Liu Z, Liu Y, Sun Y, Chen G, Chen Y. Double-stranded DNA-scaffolded fluorescent probes for fluorescence imaging of cell-surface molecules. *RSC advances* [internet]. 2017 [cited 2021] 7(83):52581-7. Available from: <https://doi.org/10.1039/C7RA09869C>
70. Sedlak SM, Schendel LC, Gaub HE, Bernardi RC. Streptavidin/biotin: Tethering geometry defines unbinding mechanics. *Science Advances* [internet]. 2020 Mar 25 [cited 2021] 6(13):eaay5999. Available from: <https://doi.org/10.1126/sciadv.aay5999>

71. Berg TJ, Stryer L. A nucleic acid consists of four kinds of bases linked to a sugar-phosphate backbone. *Biochemistry* [internet]. 5th ed. New York: W H Freeman and company; 2002 [cited 2021]. Available from: <https://www.ncbi.nlm.nih.gov/books/NBK22490/>
72. Tuzikov A, Chinarev A, Shilova N, Gordeeva E, Galanina O, Ovchinnikova T, et al. 40 years of glyco-polyacrylamide in glycobiology. *Glycoconjugate Journal* [internet]. 2021 Jan [cited 2021] 38(1):89-100. Available from: <https://doi.org/10.1007/s10719-020-09965-5>
73. Nagappan R, Flegel WA, Srivastava K, Williams EC, Ryzhov I, Tuzikov A, et al. COVID-19 antibody screening with SARS-CoV-2 red cell kodecytes using routine serologic diagnostic platforms. *Transfusion* [internet]. 2021 April [cited 2021] 61(4):1171-80. Available from: <https://doi.org/10.1111/trf.16327>
74. Alikhani A, Korchagina EY, Chinarev AA, Bovin NV, Federspiel WJ. High molecular weight blood group A trisaccharide-polyacrylamide glycoconjugates as synthetic blood group A antigens for anti-A antibody removal devices. *Journal of Biomedical Materials Research* [internet]. 2009 Nov [cited 2021] 91(2):845-54. Available from: <https://pubmed.ncbi.nlm.nih.gov/19582848/>
75. Qiu J, Wang C. ABO Blood Group Antibodies. *ABO-incompatible Organ Transplantation* [internet]. 2019 February [cited 2021] 37-63. Available from: https://link.springer.com/chapter/10.1007/978-981-13-3399-6_3
76. Perry H. Development of Novel Carbohydrate Blood Group Related Kodecyte Assays 2019 [dissertation on internet] New Zealand: Auckland university of technology; 2019 [cited 2021]. Available from: <http://hdl.handle.net/10292/12923>
77. Giron K. EC. A Practical Guide to Analyzing Nucleic Acid Concentration and Purity with Microvolume Spectrophotometers. *New England Biolabs* [internet]. 2019 [cited 2021]. Available from: <https://www.bioke.com/support/appnotes/1345/a-practical-guide-to-analyzing-nucleic-acid-concentration-and-purity-with-microvolume-spectrophotometers.html>
78. Agilent Technologies. Agilent High sensitivity DNA Kit Guide [internet]. Germany: Agilent Technologies; 2013 [updated 2009;cited 2021]. Available from: https://www.agilent.com/cs/library/usermanuals/Public/G2938-90321_SensitivityDNA_KG_EN.pdf.
79. Kit YS, Chandran S. A simple, rapid and efficient method of isolating DNA from Chokanan mango (*Mangifera indica* L.). *African Journal of Biotechnology* [internet]. 2010 Sep [cited 2021] 9(36): 5805-5808. Available from: <https://www.ajol.info/index.php/ajb/article/view/92791>
80. Desjardins P, Conklin D. NanoDrop microvolume quantitation of nucleic acids. *Journal of Visualized Experiments* [internet]. 2010 Nov 22 [cited 2021] (45):e2565. Available from: <https://doi.org/10.3791/2565>
81. Misumi M, Weissbach A. The isolation and characterization of DNA polymerase alpha from spinach. *Journal of Biological Chemistry* [internet]. 1982 Mar 10 [cited 2021] 257(5):2323-9. Available from: [https://doi.org/10.1016/S0021-9258\(18\)34925-1](https://doi.org/10.1016/S0021-9258(18)34925-1)

82. El-Bali L, Diman A, Bernard A, Roosens NH, De Keersmaecker SC. Comparative study of seven commercial kits for human DNA extraction from urine samples suitable for DNA biomarker-based public health studies. *Journal of biomolecular techniques* [internet]. 2014 [cited 2021];25(4):96. Available from: [10.7171/jbt.14-2504-002](https://doi.org/10.7171/jbt.14-2504-002)
83. Natarajan VP, Zhang X, Morono Y, Inagaki F, Wang F. A modified SDS-based DNA extraction method for high quality environmental DNA from seafloor environments. *Frontiers in microbiology* [internet]. 2016 Jun 23 [cited 2021]7:986. Available from: <https://doi.org/10.3389/fmicb.2016.00986>
84. Goldenberger D, Perschil I, Ritzler M, Altwegg M. A simple "universal" DNA extraction procedure using SDS and proteinase K is compatible with direct PCR amplification. *Genome Research* [internet]. 1995 Jun 1 [cited 2021] 4(6):368-70. Available from: <https://doi.org/10.1101/GR.4.6.368>
85. Chacon-Cortes D, Griffiths LR. Methods for extracting genomic DNA from whole blood samples: current perspectives. *Journal of biorepository science for applied medicine* [internet]. 2014 May 28 [cited 2021] 2:1-9. Available from: <https://www.dovepress.com/getfile.php?fileID=20256>
86. DDi PF, Ortenzi F, Tilio M, Concetti F, Napolioni V. Genomic DNA extraction from whole blood stored from 15-to 30-years at– 20 °C by rapid phenol–chloroform protocol: A useful tool for genetic epidemiology studies. *Molecular and cellular probes* [internet]. 2011 Feb 1 [cited 2021] 25(1):44-8. Available from: <https://doi.org/10.1016/j.mcp.2010.10.003>
87. Zheng G, Czaplá L, Srinivasan AR, Olson WK. How stiff is DNA? *Physical Chemistry Chemical Physics* [internet]. 2010 [cited 2021] 12(6):1399-406. Available from: <https://doi.org/10.1039/B916183J>
88. Chodosh LA. Purification of DNA-Binding Proteins Using Biotin/Streptavidin Affinity Systems. *Current protocols in molecular biology* [internet]. 1996 Oct [cited 2021]36(1):12-6. Available from: <https://doi.org/10.1002/0471142727.mb1206s36>
89. Xu H, Zhang S, Liu D, Liang CC. End-labeling of long DNA fragments with biotin and detection of DNA immobilized on magnetic beads. *Molecular biotechnology* [internet]. 2001 Feb [cited 2021] 17(2):183-5. Available from: <https://link.springer.com/content/pdf/10.1385/MB:17:2:183.pdf>
90. Urrechaga E, Borque L, Escanero J. Analysis of reticulocyte parameters on the Sysmex XE 5000 and LH 750 analyzers in the diagnosis of inefficient erythropoiesis. *International journal of laboratory haematology* [internet]. 2011 [cited 2021](1):37. Available from: [10.1111/j.1751-553X.2010.01238.x](https://doi.org/10.1111/j.1751-553X.2010.01238.x)
91. Heath CW, Daland GA. Staining of reticulocytes by brilliant cresyl blue: influence of solutions of substances. *Archives of Internal Medicine* [internet]. 1931 Jul 1 [cited 2021] 48(1):133-45. Available from: <https://doi.org/10.1001/archinte.1931.00150010138009>
92. Tatsumi N, Tsuda I. Marked changes in red cell volume response to isotonic glucose solution during storage. *Haematologia* [internet]. 1987 Jan 1 [cited 2021] 20(2):67-72. Available from: <https://europepmc.org/article/med/3653790>

93. Orlov D, Karkouti K. The pathophysiology and consequences of red blood cell storage. *Anaesthesia* [internet]. 2015 Jan [cited 2021] 70:29-e12. Available from: <https://doi.org/10.1111/anae.12891>
94. Zheng H, Chen XL, Zhu CQ, Li DH, Chen QY, Xu JG. Brilliant cresyl blue as a new red region fluorescent probe for determination of nucleic acids. *Microchemical journal* [internet]. 2000 May 15 [cited 2021] 64(3):263-9. Available from: [https://doi.org/10.1016/S0026-265X\(00\)00015-1](https://doi.org/10.1016/S0026-265X(00)00015-1)

Glossary of Medical and Scientific Terms

CH ₃ COONa	Sodium Acetate
DNA	Deoxyribose Nucleic Acid
DiOCI	3,3'- dimethyloxacarbocyanine
EDTA	Ethylenediaminetetraacetic acid
ELISA	Enzyme-Linked Immune Sorbent Assay
ICHS	International Council of Standardisation in Haematology
KCl	Potassium Chloride
KH ₂ PO ₄	Potassium Dihydrogen Phosphate
mol/L	Milli Moles per Liter
Na ₂ HPO ₄ .2H ₂ O	Disodium Phosphate
NaCl	Sodium Chloride
NaHCO ₃	Sodium Bicarbonate
NH ₄ CH ₃ CO ₂	Ammonium Acetate
NH ₄ Cl	Ammonium Chloride
PBS	Phosphate Buffered Saline
RBC	Red Blood Cell
RNA	Ribonucleic Acid
SDS	Sodium Dodecyl Sulphate
TRIS	Trisaminomethane
UV	Ultraviolet
WBC	White Blood Cell